Journal of Archaeological Science 70 (2016) 102–116

Contents lists available at ScienceDirect

Journal of Archaeological Science

journal homepage: http://www.elsevier.com/locate/jas

Improvement of laser ablation *in situ* micro-analysis to identify diagenetic alteration and measure strontium isotope ratios in fossil human teeth

M. Willmes [a, *], L. Kinsley [a], M.-H. Moncel [b], R.A. Armstrong [a], M. Aubert [a, 1], S. Eggins [a], R. Grün [a, 2]

[a] Research School of Earth Sciences, The Australian National University, Canberra ACT 2601, Australia
[b] Département de Préhistoire, Muséum National d'Histoire Naturelle, CNRS UMR 7194, 1 Rue René Panhard, France

ARTICLE INFO

Article history:
Received 19 November 2015
Received in revised form
5 February 2016
Accepted 12 April 2016

Keywords:
Strontium isotopes
Laser ablation MC-ICP-MS
Diagenetic overprint
In situ analysis
Human mobility

ABSTRACT

Strontium isotope ratios measured in fossil human teeth are a powerful tool to investigate past mobility patterns. In order to apply this method, the sample needs to be investigated for possible diagenetic alteration and a least destructive analytical technique needs to be employed for the isotopic analysis. We tested the useability of U, Th, and Zn distribution maps to identify zones of diagenetic overprint in human teeth. Areas with elevated U concentrations in enamel were directly associated with diagenetic alterations in the Sr isotopic composition. Once suitable domains within the tooth are identified, strontium isotope ratios can be determined either with micro-drilling followed by TIMS analysis or *in situ* LA-MC-ICP-MS. Obtaining accurate $^{87}Sr/^{86}Sr$ isotope ratios from LA-MC-ICP-MS is complicated by the potential occurrence of a significant direct interference on mass 87 from a polyatomic compound. We found that this polyatomic compound is present in our analytical setup but is Ar rather than Ca based, as was previously suggested. The effect of this interference can be significantly reduced by tuning the instrument for reduced oxide levels. We applied this improved analytical protocol to a range of human and animal teeth and compared the results with micro-drilling strontium isotopic analysis using TIMS. Tuning for reduced oxide levels allowed the measurement of accurate strontium isotope ratios from human and animal tooth enamel and dentine, even at low Sr concentrations. The average offset between laser ablation and solution analysis using the improved analytical protocol is 38 ± 394 ppm ($n = 21$, 2σ). LA-MC-ICP-MS thus provides a powerful alternative to micro-drilling TIMS for the analysis of fossil human teeth. This method can be used to untangle diagenetic overprint from the intra-tooth isotopic variability, which results from genuine changes in $^{87}Sr/^{86}Sr$ isotope ratios related to changes in food source, and by extension mobility.

1. Introduction

Radiogenic strontium isotope compositions ($^{87}Sr/^{86}Sr$) of human and animal skeletal remains can be used to reconstruct their habitat use and ranging patterns (Bentley, 2006; Price et al., 2002; Slovak and Paytan, 2012). Radiogenic strontium isotope ratios vary between different regions, primarily depending on the age and composition of the underlying geology, augmented by external processes such as precipitation, seaspray, and dust (Bentley, 2006; Capo et al., 1998; Evans et al., 2010; Maurer et al., 2012; Montgomery et al., 2007; Sillen et al., 1998). Strontium enters the body through diet, substitutes for calcium in biological apatite, which is used in the formation of bones and teeth, and serves no metabolic function. Therefore, the $^{87}Sr/^{86}Sr$ isotope ratio measured in skeletal remains will reflect the concentration-weighted average of dietary Sr, that was consumed while the skeletal tissue was formed (Beard and Johnson, 2000; Bentley, 2006). Thus, $^{87}Sr/^{86}Sr$ isotope ratios can be used to reconstruct change in food source and by extension residence area. A common problem when working

* Corresponding author.
E-mail address: malte.willmes@googlemail.com (M. Willmes).
[1] Now at: Research Centre of Human Evolution, Environmental Futures Research Institute, Griffith University, Gold Coast, Queensland 4222, Australia.
[2] Now at: Research Centre of Human Evolution, Environmental Futures Research Institute, Griffith University, 170 Kessels Road, Nathan, Queensland 4111, Australia.

http://dx.doi.org/10.1016/j.jas.2016.04.017
0305-4403/

with fossils remains is that diagenetic processes can change the original isotope compositions, rendering the sample unsuitable for isotopic provenance studies. In addition, isotopic analyses are often destructive, which prohibits their application to valuable fossil remains. Laser ablation multi-collectorinductively coupled plasma mass spectrometry (LA-MC-ICP-MS) is an analytical method that has the potential to overcome both of these limitations, because it allows for rapid *in situ* screening for diagenetic overprints, and least-destructive strontium isotope analysis of the same sample (Benson et al., 2013; Grün et al., 2014). In this paper, we outline a method to investigate diagenetic overprinting in fossil teeth using U, Th, and Zn concentration distribution maps. We then tested our protocol for $^{87}Sr/^{86}Sr$ isotope analysis in teeth in regard to the current limitations in terms of accuracy and precision, which have been observed in a significant number of analytical facilities, and are hypothesised to be mainly caused by a polyatomic interference on mass 87 (Horstwood et al., 2008; Lewis et al., 2014).

1.1. Diagenetic alteration of fossil teeth

The formation of human tooth enamel and dentine of the permanent dentition is a complex process beginning *in utero* (Ash and Nelson, 2003; Nanci, 2012). The mineral component of teeth is bioapatite, which is similar to hydroxyapatite, but affected by numerous substitutions of the Ca, PO_4, and OH groups with secondary groups, such as Sr, Mg, and Ba. These secondary groups are subject to biological selection and vary in concentration with changes in trophic levels, between different species, and with the element abundance in the underlying substrate (Burton and Wright, 1995; Elliott, 2002). Intra-tooth measurements in mammals may be used to connect the intra tooth isotopic variations to mobility (Balasse et al., 2002; Britton et al., 2009). In human teeth, enamel does not remodel after formation and is closed to chemical exchange (Nanci, 2012). Thus, intra-tooth isotopic variations may relate to the sequential mineralisation of the tooth enamel. However, while the timing of tooth development in humans is well constrained, the complex pattern, timing and rates of mineralisation and maturation of tooth enamel are currently not completely resolved (Balasse, 2002; Montgomery et al., 2012; Suga, 1989).

The preservation of skeletal remains depends on their environmental surroundings. Diagenetic alterations are a common problem for many archaeological samples. To ensure that the isotopic ratios measured in a tooth reflect the original isotopic composition, it is important to identify the domains within the tooth that are least affected by diagenetic alteration (Nelson et al., 1986). For the investigation of diagenetic changes in tooth enamel, a variety of methods have been used, including infra-red (IR) spectroscopy (Sponheimer and Lee-Thorp, 1999) and cathodoluminescence (CL) imaging (Schoeninger et al., 2003). Nearly all of these studies have employed bulk analysis with the aim of testing cleaning techniques (Hoppe et al., 2003; Price et al., 1992; Trickett et al., 2003) or coarse sub-sampling using mineralogical information (e.g. by CL) as a guide. While these approaches provide some information as to the mineralogical state of the hydroxyapatite or functional groups within this mineral (such as hydroxyl or phosphate), any conclusions about sample integrity for isotopic analysis are derived from conjecture. Mapping of element distributions has been used to identify the degree of diagenesis in bones (Fernandes et al., 2013; Koenig et al., 2009; Trueman et al., 2008). In addition, a few studies have investigated the mechanisms of diagenetic alteration using high resolution elemental or isotope analysis (Jacques et al., 2008; Kohn et al., 1999; Martin et al., 2008; McCormack et al., 2015).

Systematic mapping of U, Th, and Zn concentrations may help to qualitatively identify domains of diagenetic alteration in skeletal materials. The basic principle is that modern teeth and bones contain only trace amounts of uranium and thorium and thus their presence in archaeological skeletal remains can be used to identify zones of diagenetic overprinting (Boel, 2011; Budd et al., 2000; Eggins et al., 2003; Grün et al., 2008; Hinz and Kohn, 2010; Koenig et al., 2009). Uranium is water soluble and highly mobile in skeletal tissues and consequently its concentration and spatial distribution are highly variable and can change on small scales on the order of tens of μm (Duval et al., 2011; Grün et al., 2008, 2014). Thorium, on the other hand, is water insoluble and represents mechanical overprinting of the sample, for example by clay particles in pores and on the surface. However, there is no linear correlation between uranium and thorium incorporation and the uptake of other elements, such as Sr. This hinders the quantification of possible Sr overprint based on the distributions of U and Th. Nevertheless, zones within a tooth showing high U or Th concentrations can indicate diagenetic overprints, while zones with low U and Th concentrations are more likely to preserve the original Sr isotope ratio. In mammals, low U zones often occur close to the surface of the tooth enamel, within 200–400 μm (Boel, 2011; Budd et al., 2000; Eggins et al., 2003; Grün et al., 2008). The first aim of this research paper is to further test this screening method and to evaluate the usefulness of Zn as an additional tracer to identify zones, which have retained the original strontium isotopic compositions.

1.2. Strontium isotope analysis of fossil teeth

Strontium isotope ratios from fossil teeth can be analysed either using sample dissolution followed by mass spectrometric measurements (thermal ionisation mass spectrometry (TIMS) or multi-collector inductively coupled plasma mass spectrometry (MC-ICP-MS)), or *in situ* using laser ablation (LA)-MC-ICP-MS. For solution analyses, a micro-drill can be used to extract a small amount of sample, which is then digested in acid and Sr is separated from the matrix elements using ion exchange chromatography. This technique is accurate and reliable, but also time intensive and potentially more destructive to the sample than *in situ* LA-MC-ICP-MS. The amount of material required varies between a few μg to several tens of mg depending on the Sr concentration, drill setup, and instrument capacity. For samples requiring more than 0.5 mg, drilling causes large destructive marks on the sample, making this technique unsuitable for valuable archaeological materials. Micro-drilling smaller amounts of sample <0.1 mg is much less destructive, but it is also technically challenging and the equipment is not widely available (e.g., Charlier et al., 2006). LA-MC-ICP-MS allows *in situ* analysis of a sample and has shown great potential in analysing skeletal remains because it is fast, requires minimal sample preparation, and provides high spatial resolution (50–200 μm). Additionally, this method allows for large numbers of measurements on the same skeletal fragment to test for compositional variability within the same specimen. Traditionally, samples were cut to create a flat sample surface for laser ablation analysis, which creates significant damage. However, recent studies have shown that accurate data can also be obtained from the outer uncut sample surface (Benson et al., 2013; Copeland et al., 2011; Le Roux et al., 2014).

Problems with laser ablation analysis of the $^{87}Sr/^{86}Sr$ isotope ratios in fossil skeletal material result from molecular interferences from Ca, Kr, Ar, and Rb, that can severely limit the accuracy and precision (Copeland et al., 2008; Horstwood et al., 2008; Paton et al., 2007; Simonetti et al., 2008; Vroon et al., 2008; Woodhead et al., 2005). In particular, the occurrence of a direct interference on mass 87 from a polyatomic compound, possibly $^{40}Ca^{31}P^{16}O$, has been suggested to be the main cause for

the consistent positive offsets, observed in a significant number of analytical facilities, between the $^{87}Sr/^{86}Sr$ isotope ratios measured with LA-MC-ICP-MS and with solution methods ($\Delta_{LA\text{-}TIMS}$) on the order of 500–1500 ppm (Horstwood et al., 2008; Lewis et al., 2014; Simonetti et al., 2008). The effect of this polyatomic interference on the $^{87}Sr/^{86}Sr$ isotope ratio was found to be highest in samples with low Sr concentration, relative to Ca and P (Horstwood et al., 2008; Simonetti et al., 2008). The Sr/Ca ratio in biogenic apatite is controlled by the Sr concentration because calcium is a stoichiometric component and can thus be treated as constant. It follows, that under constant laser sampling ablation conditions, the effect of the polyatomic interference on the $^{87}Sr/^{86}Sr$ ratio varies in proportion with changes in Sr concentration (Horstwood et al., 2008). The effect of this interference on samples with high Sr concentration (e.g. >1500 ppm) is minimal (Simonetti et al., 2008), however, most human tooth samples have much lower Sr concentrations, in the range of 50 ppm–500 ppm (Bentley, 2006). An isotopically homogenous tooth that has varying Sr concentrations could then show varying $^{87}Sr/^{86}Sr$ isotope ratios when this interference is not corrected for adequately (Horstwood et al., 2008; Nowell and Horstwood, 2009; Richards et al., 2009; Simonetti et al., 2008).

Several methods have been tested to increase the accuracy of LA-MC-ICP-MS analyses on human teeth. Horstwood et al. (2008) used samples with known $^{87}Sr/^{86}Sr$ isotope ratios to calibrate the LA-MC-ICP-MS analyses but found that this approach limited the precision of the analysis. Tuning for reduced oxide levels has been successful in reducing $\Delta_{LA\text{-}TIMS}$ to 600–100 ± 100 ppm (de Jong et al., 2007; Foster and Vance, 2006). A recent study by Lewis et al. (2014) combined tuning for reduced oxide levels with a customized plasma interface. Their setup is similar to a collision cell and allowed for the addition of a variable He flow after the skimmer cone, requiring minimal modification of the mass spectrometer. Using tuning for reduced oxide levels they achieved an accuracy of 100–600 ppm in bone and tooth enamel, which improved to 30 ± 50 ppm with the addition of the customized plasma interface. Their analytical setup reduced the signal intensity by only 20–30% and thus is highly applicable to samples with low strontium concentration, such as human teeth. However, modification of the plasma interface is not always possible at an analytical facility with a broad range of applications of different isotopic systems. The second aim of this paper is to further investigate the causes of the polyatomic interference on mass 87 and evaluate our analytical protocol to reduce its effect on the measurement of $^{87}Sr/^{86}Sr$ ratios in fossil human teeth.

2. Materials and methods

2.1. Sample materials

Diagenetic overprinting was investigated using a modern human tooth, a M3 extracted from R. Grün, and a prehistoric Neanderthal tooth (Payre 1), which is an unerupted molar of an approximately three-year-old child. Detailed U and U-series maps of the Neanderthal tooth were published by Grün et al. (2008). $^{87}Sr/^{86}Sr$ isotope ratios were measured both with solution TIMS and *in situ* LA-MC-ICP-MS. TIMS results are taken here to represent the true value against which the LA-MC-ICP-MS results are compared. Samples were taken from the same locations within each tooth. These samples include eight teeth from Le Tumulus des Sables (Boel, 2011; Courtaud et al., 2010), four Neanderthal teeth from the site of Payre in France, one bovid tooth from Holon, Israel (Benson et al., 2013; Porat et al., 1999) and a diprotodon molar from Camel Swamp, Australia (Benson et al., 2013). We also measured modern marine teeth from a grey nurse shark (*Carcharias taurus*) and a dugong (*Dugong dugon*). In addition, the strontium carbonate standard SRM987 (National Institute of Standards and Technology) was used to mix a series of standard solutions containing varying concentrations of P using the 1000 ppm Phosphorus AccuTrace Reference Standard. A solution of 2% nitric acid in MilliQ, was mixed with varying concentrations of P and Ca + P (1:1 to 1:0.05) in order to create an additional standard solution.

2.2. Thermal ionisation mass spectrometry (TIMS)

After cleaning the surface of the teeth, 0.2–0.5 mg of material was drilled out using a 0.3 mm custom made drill bit at 500 rpm. The samples were then leached in 0.5 ml 1 M ammonium nitrate to remove any residual contamination and digested in 1 ml concentrated nitric acid for 1 h. The samples were then evaporated to dryness, redissolved in 2 ml 2 M nitric acid and subjected to ion exchange chromatography using 50 μl columns with Eichrom Sr specific resin (pre-filter and Sr spec resin) to isolate Sr from other elements (Horwitz et al., 1992). A drop of diluted phosphoric acid was added to each sample before loading onto rhenium filaments with a TaF_5 activator. Samples were measured on a TRITON Plus thermal ionisation mass spectrometer (TIMS) at the Research School of Earth Sciences, ANU. Data reduction procedures include Rb correction ($^{85}Rb/^{87}Rb = 2.591$), exponential mass bias correction ($^{86}Sr/^{88}Sr$ ratio of 0.1194), and 2σ outlier rejection. Total procedural blanks were determined by isotope dilution using a ^{84}Sr enriched spike, measured on the TRITON Plus TIMS and are below 100 pg Sr. This blank contribution is insignificant compared to the amount of sample Sr measured (>100 ng). Long term measurements of the Sr carbonate standard SRM987 (National Institute of Standards and Technology) gave an average $^{87}Sr/^{86}Sr$ value of 0.71023 ± 2 (n = 99, 2σ), which is in agreement with the original certified $^{87}Sr/^{86}Sr$ isotope value of 0.71034 ± 26 (Moore et al., 1982) as well as the more commonly quoted accepted value of 0.71025 ± 1 (Hans et al., 2013; McArthur, 1994; Thirlwall, 1991).

2.3. Laser ablation analysis

Samples were prepared by cutting along the buccal-lingual (cheek to tongue) axis using a fine diamond saw (100 μm) to produce a flat surface exposing both the enamel and dentine. Two of the Neanderthal teeth (Payre 2, 3) and the shark and dugong teeth were analysed from the outside without cutting. The *in situ* elemental and isotopic analyses were carried out using a custom-built laser ablation sampling system (ANU HelEx) interfaced with an ArF Excimer laser (193 nm; Lambda Physik Compex 110) and ICP-MS and MC-ICP-MS. Details of the ANU system and its capabilities have been described in detail previously (Eggins et al., 1998, 2003). In brief, it employs a single long-working distance lens to project and demagnify (by a factor of 20) the image of a laser-illuminated aperture onto the sample surface, which enables a range of geometries to be ablated within bounding dimensions of between about 5 μm and 400 μm. Samples were mounted so that their surface is positioned in the focal plane of the laser. In this study laser pulse rates of 5 and 10 Hz were employed with a fluence of 10 J/cm^2 (power density 0.3 GW/cm^2), the latter resulting in removal of a uniformly thick layer (≈200 nm) from the targeted sample site with each laser pulse. The in-house developed laser ablation cell produces very fast response times, which permits high spatial resolution analysis. Laser ablation was performed under a pure helium atmosphere with a continuous flow of 500 cm^3 min^{-1} through the cell. After the cell, approximately 1 l min^{-1} argon is added to the gas

stream and is adjusted to optimise ionisation conditions.

2.3.1. Element distributions

Element concentrations were measured with a Varian-820 quadrupole ICP-MS. The maps presented here are part of a larger study that measured 58 elements in fossil and modern human teeth (Grün et al., 2013). Pre-cleaning was performed using a 230 μm spot scanned at 100 μm/s across the sample surface, with the laser operating at 10 pulses per second. For elemental analysis, a track with a spot size of 100 μm with laser pulse rates of 10 Hz was employed. The NIST reference glasses SRM610 and SRM612 were used as calibration standards for element concentration determinations. Data reduction for elemental analysis followed Longerich et al. (1996) and involved the subtraction of interpolated plasma background intensities, measured before and after analysis of the sample. Signal intensities were normalised to ^{43}Ca for each time slice, drift corrected relative to the NIST standard measured before and after the sample sequence, and then calibrated with respect to the known element ratios of the NIST610 and NIST612 standards. Reference data for the NIST standards (Jochum et al., 2011) were taken from the GeoRem database (http://georem.mpch-mainz.gwdg.de).

2.3.2. Strontium isotope measurements

For *in situ* ^{87}Sr/^{86}Sr isotope analysis, the laser ablation-system was connected to a Neptune MC-ICP-MS with Faraday cup detectors set to measure three different sequences in dynamic mode (Table 1), thus allowing for monitoring of all identified potential interferences (Table 2). Spot sampling measurements were performed for isotope analyses, with a sample ablation time of 60 s, using a 180 μm diameter spot and the laser operating with a pulse frequency of 5 Hz. Typical operating conditions are shown in Table 3. To remove any surface contamination produced during the sample preparation process, including settled dust and fine particles, the samples were first subjected to a cleaning run using a laser spot of 265 μm for 10 s. Faraday detector integration times were 5 s. An in-house Sr standard, consisting of a piece of modern Giant Clam (*Tridacna gigas*) from the Great Barrier Reef, was measured 3 times before and after each sample analytical sequence to monitor for instrument drift during the analytical session. For the modern Giant Clam, we obtained an average Sr isotope composition of 0.70920 ± 6 (n = 153, 2σ), which is consistent with present-day values of seawater (McArthur et al., 2001).

2.3.3. Interference correction protocol

A number of methods have been used to account and correct for the different interferences present when analysing strontium isotopes using LA-MC-ICP-MS (Vroon et al., 2008). The relevant interferences on LA-MC-ICP-MS analysis of Sr in skeletal tissue are shown in Table 2. The potential isobaric interferences on the ^{87}Sr/^{86}Sr ratio are double charged rare earth elements (REEs), Kr, Rb, Ca dimers, and polyatomic interferences (Horstwood et al., 2008; Müller and Anczkiewicz, 2016; Paton et al., 2007; Simonetti et al., 2008; Vroon et al., 2008; Woodhead et al., 2005). Since some of the corrections required use mass peaks that have pre-existing interferences, the order in which the corrections are applied is important and is discussed below. All isotope ratios used were taken from Rosman and Taylor (1998). Table 4 lists average elemental concentrations in tooth enamel for a variety of elements for the assessment of possible interferences.

2.3.3.1. Background levels. Background levels were monitored before and after each measurement using the same instrument conditions as during analysis, except without ablating material. Washout times of ~60 s are long enough to ensure that no wash-out effects, e.g. from the previous sample, are present and typical blank levels are shown in Table 5.

2.3.3.2. Rare earth elements. Significant interferences from REE elements may occur due to the formation of doubly charged REE species (Paton et al., 2007). REE concentrations in skeletal material are generally low, however, post burial uptake can occur (Trueman and Tuross, 2002; Trueman et al., 2011). The measured intensities at half masses 81.5, 83.5, 85.5 and 86.5 are used to monitor ^{163}Dy^{++}, ^{167}Er^{++}, ^{171}Yb^{++}, ^{173}Yb^{++}, respectively. The signals could be used to subtract the appropriate amounts of relevant double charged on-peak interferences from all Sr peaks. As can be seen in Table 4, these REE are close to background in both the modern and fossil samples. Should significant REE signals occur, this would be a sign of either diagenetic alteration or incomplete cleaning (some polishing pastes contain high REE and W concentrations). Such samples should be checked and rerun or removed from further analysis. ^{89}Y was used as the primary indicator for the presence of REE in teeth. ^{89}Y is a sensitive indicator of potential REE interference because it is chemically similar to the lanthanide REEs, and is generally concentrated in minerals that contain REEs. In addition, doubly charged REEs would be several orders of magnitude lower than the single charged species.

2.3.3.3. Ca dimers and argides. Samples with high Ca concentrations may produce calcium dimers and calcium argides in the plasma. ^{40}Ca^{44}Ca, ^{40}Ca^{46}Ca and ^{40}Ca^{48}Ca dimers interfere with the ^{84}Sr, ^{86}Sr and ^{88}Sr, respectively. To correct for these the Ca dimer intensity on mass 82 was measured. However, on this mass there is a ^{82}Kr interference, which is monitored on mass 83 and calculated using the known ^{83}Kr/^{82}Kr ratio. ^{82}Kr was then subtracted from the total intensity at mass 82, leaving the ^{40}Ca^{42}Ca or ^{40}Ar^{42}Ca interferences. Using the known isotopic ratio for ^{42}Ca/^{44}Ca, ^{42}Ca/^{46}Ca, and ^{42}Ca/^{48}Ca all dimer and argide interferences could be corrected. In this experiment we did not observe any significant influence from Ca dimers or argides.

2.3.3.4. Polyatomic interferences. Both ^{40}Ca^{31}P^{16}O and ^{40}Ar^{31}P^{16}O may interfere on mass 87 when measuring calcium phosphate matrices. This interference is investigated in this study and discussed in detail in the results and discussion section.

Table 1
Cup configuration of the LA-MC-ICP-MS for strontium isotope measurements of skeletal remains at RSES.

	L4	L3	L2	L1	C	H1	H2	H3	H4	Integration time (s)
Seq. 1	–	82	83	84	85	86	87	88	89	5
Seq. 2	–	81.5	82.5	83.5	84.5	85.5	86.5	87.5	88.5	5
Seq. 3					71					3
Seq. 4					103.9					3

Table 2
Summary of relevant isotopes of this study and their interferences (adapted from Horstwood et al., 2008).

89	88	87.5	87	86.5	86	85.5	85	84.5	84	83.5	83	82.5	82	**81.5**	**81**
	Sr		Sr Rb		Sr		 Rb		Sr						
Y	Lu^{2+} ^{40}Ca ^{48}Ca	Lu^{2+}	Yb^{2+} $^{40}Ca^{31}P^{16}O$ $^{40}Ar^{31}P^{16}O$	Yb^{2+}	Kr Yb^{2+} ^{40}Ca ^{46}Ca	Yb^{2+}	Yb^{2+} Er^{2+}	Tm^{2+}	Kr Yb^{2+} Er^{2+} ^{40}Ca ^{44}Ca	Er^{2+}	Kr Er^{2+}	Ho^{2+}	Kr Er^{2+} Dy^{2+} ^{40}Ca ^{42}Ca	Dy^{2+}	Ar_2H

Table 3
Instrument operating conditions for *in situ* Sr isotope measurements.

Neptune MC-ICP-MS	
Forward power	1200 W
Extraction voltage	−2000 V
Analyser pressure	<5e-8 mbar
Cones	Jet sampler + standard skimmer (both Nickel)
Gas flows	
Plasma gas	17 l/min
Auxiliary gas	1 l/min
Nebuliser gas	~1 l/min
HelEx laser ablation system	
ArF Excimer laser, Lambda Physik Compex 110	193 nm
Laser fluence	~10 J/cm^2
Repetition rate	5 Hz
He gas to cell	500 ml/min

Table 4
Average elemental concentrations measured in the enamel of a modern tooth (RG) and a Neanderthal tooth from Payre (from Grün et al., 2013). DL stands for detection limit.

	Sr (ppm)	Rb (ppb)	Y (ppb)	Dy (ppb)	Ho (ppb)	Er (ppb)	Tm (ppb)	Yb (ppb)	Lu (ppb)	U (ppb)
RG	100.0 ± 0.2	299 ± 1.0	15 ± 2	1.4 ± 0.2	0.20 ± 0.04	0.7 ± 0.1	0.11 ± 0.03	9.7 ± 0.1	0.15 ± 0.02	1.0 ± 0.1
Neanderthal	151.3 ± 3.6	232 ± 1.8	19 ± 1	2.2 ± 0.3	0.41 ± 0.08	<DL	0.22 ± 0.06	1.8 ± 0.3	0.20 ± 0.08	625 ± 7.8

2.3.3.5. Mass bias. The isotopic fractionation induced from the laser and the instrument mass discrimination are corrected during Sr isotope analyses by using an exponential correction to the stable $^{86}Sr/^{88}Sr$ ratio of 0.1194.

2.3.3.6. Krypton. Kr occurs as an impurity in the Ar gas and interferes with masses ^{84}Sr and ^{86}Sr. The amount of Kr varies depending on the gas supplier, between different batches, and also with time within a single vessel, as the Ar is used up (Woodhead et al., 2005). A standard method to correct for Kr is using a gas blank correction, measured before and after each sample to subtract the intensities (Vroon et al., 2008; Woodhead et al., 2005). A problem with this correction is the assumption that the measured Kr intensity stays the same whether or not sample material is being ablated. This is not necessarily correct, as the presence of ablated material changes the plasma loading and consequently the percentage of ionisation of atoms in the plasma. Correcting for the Kr interference using peak stripping is further complicated by the uncertainty surrounding the Kr mass bias (Jackson and Hart, 2006; Vroon et al., 2008). We used a similar approach to Jackson and Hart (2006) and corrected for the Kr interference by subtracting ^{84}Kr from mass 84 until the $^{84}Sr/^{88}Sr$ ratio reaches the known value of 0.00672, see also Konter and Storm (2014). Iterations are used for the mass bias correction, substituting the Kr number in the $^{86}Sr/^{88}Sr$ ratio and repeating the calculations until no more change in the calculated isotope ratios is observed. This removes the possibility of using the $^{84}Sr/^{86}Sr$ ratio as a data quality control. However, the $^{84}Sr/^{86}Sr$ isotope ratio, while useful as a general monitor of the correction procedures, is problematic because of the very small intensities at these masses. The precision of the $^{84}Sr/^{86}Sr$ does not necessarily reflect that of the $^{87}Sr/^{86}Sr$ ratios (Copeland et al., 2010).

Table 5
Typical blank levels after 60 s washout time.

Mass	Isotopes/polyatomic compounds	Average V (n = 30)	2se
89	^{89}Y	4.2E-06	9.2E-07
82	$^{82}Kr+^{40}Ca^{42}Ca$	1.3E-04	1.2E-05
83	^{83}Kr	8.1E-05	5.7E-06
84	$^{84}Sr + ^{84}Kr + ^{40}Ca^{44}Ca$	3.6E-04	2.8E-05
85	^{85}Rb	2.0E-05	1.3E-06
86	$^{86}Sr + ^{86}Kr + ^{40}Ca^{46}Ca$	1.5E-04	1.1E-05
87	$^{87}Sr + ^{87}Rb + ^{40}Ca^{31}P^{16}O, ^{40}Ar^{31}P^{16}O$	4.0E-05	4.1E-06
88	$^{40}Ca^{31}P, ^{40}Ar^{31}P$	1.7E-04	6.9E-06
71	$^{88}Sr + ^{40}Ca^{48}Ca$	3.2E-04	2.9E-05
104	$^{88}Sr + ^{16}O$	4.6E-05	4.0E-06

2.3.3.7. Rubidium. The direct interference of ^{87}Rb on the $^{87}Sr/^{86}Sr$ is corrected by monitoring ^{85}Rb and subtracting the appropriate amount from the signal at mass 87 assuming the natural $^{85}Rb/^{87}Rb$ ratio. The $^{85}Rb/^{87}Rb$ ratio is then reversely corrected for mass bias, using the Sr mass bias. This correction method is limited because it assumes that the mass bias for Rb and Sr are the same, which is not necessarily correct. Generally, in teeth the Rb/Sr ratio is low (see Table 4), thus this correction has a negligible effect. However, in samples with higher Rb/Sr ratio the possible difference between the Rb mass bias and Sr mass bias would have to be considered and this correction method could

have a significant effect. A recent study by Müller and Anczkiewicz (2016) was able to accurately constrain the mass bias corrected $^{85}Rb/^{87}Rb$ ratio, allowing for accurate measurements of tooth enamel with high Rb/Sr ratio.

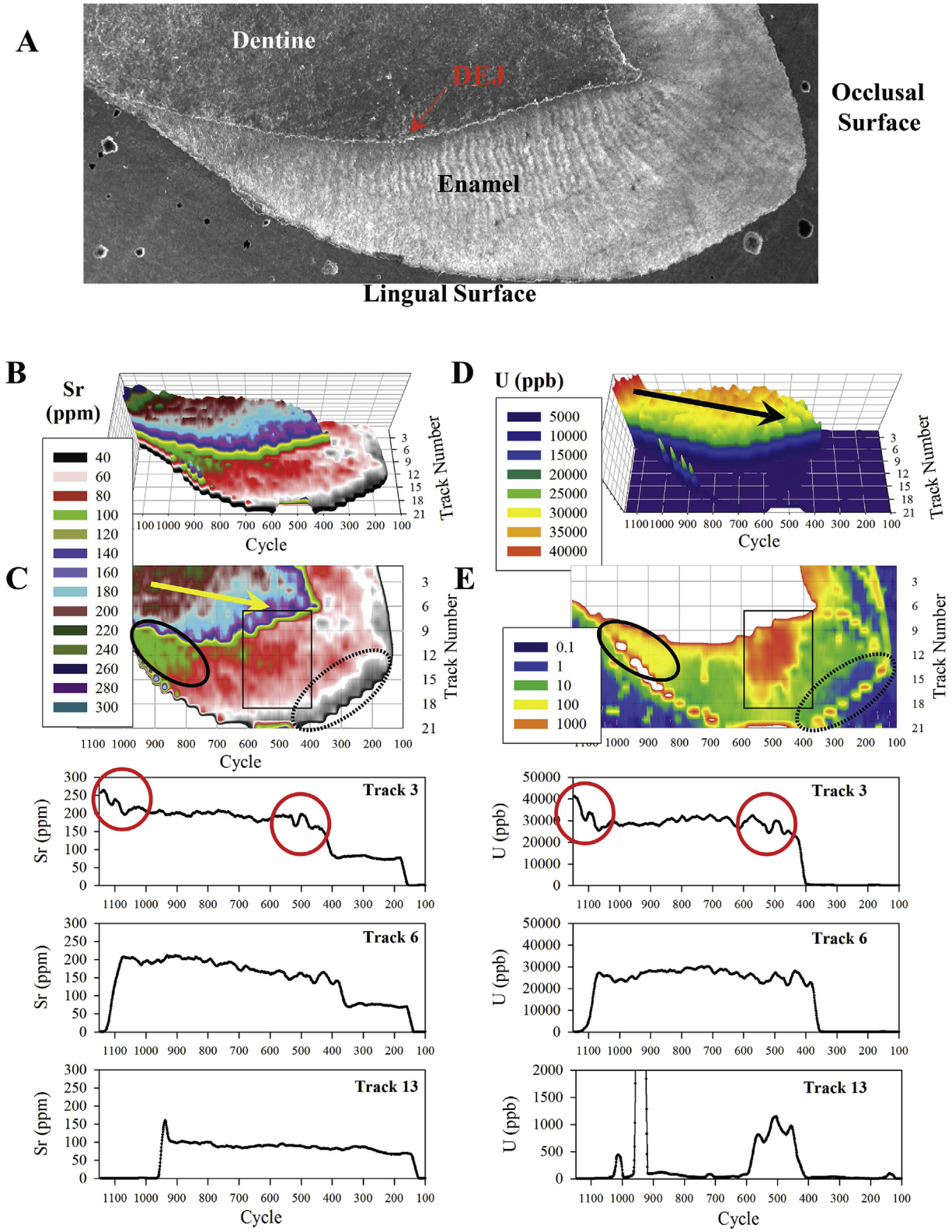

Fig. 1. Elemental distribution maps of the Neanderthal tooth (Payre 1). A: Scanning electron microscope (SEM) image of the tooth, B, C: Sr concentration maps (oblique and planar view) and selected tracks D, E: U concentration maps oblique and planar view and selected tracks. The arrow indicates a general concentration gradient. The sections indicated by circles, ellipses and rectangles are discussed in the text.

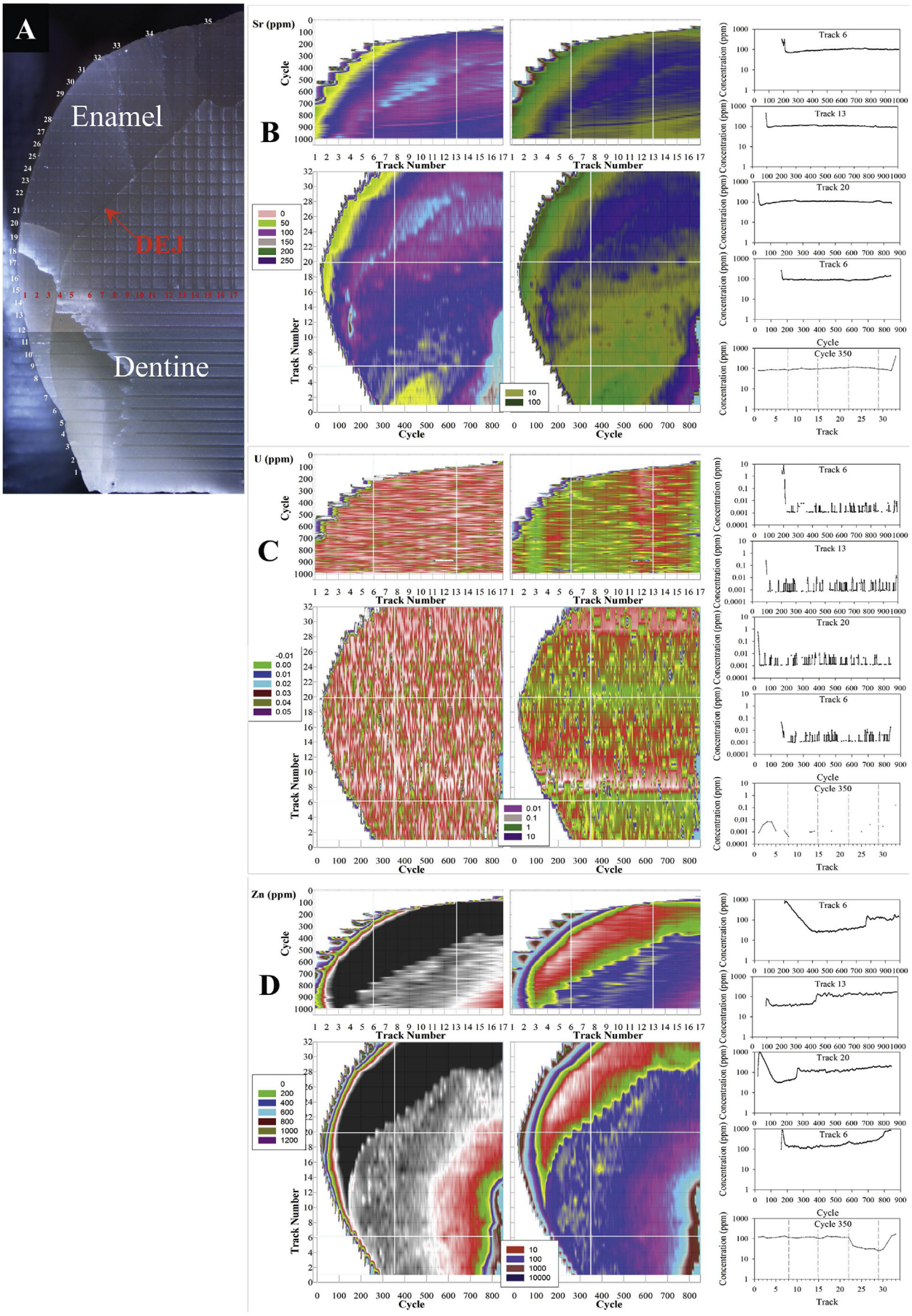

Fig. 2. Elemental distribution maps of a modern human tooth (RG), A: location of tracks, B–C: Sr, U and Zn element distribution maps (top maps: vertical tracks, below: horizontal tracks; left maps: linear scale, right maps logarithmic scale). Right hand diagrams: selected tracks indicated with the white lines in the respective maps.

3. Results and discussion

3.1. Identifying diagenetic alteration in fossil human teeth using element distribution maps

The results of the systematic mapping of elemental distribution in a Neanderthal tooth (Payre 1) and a modern human tooth (RG) and are shown in Figs. 1 and 2, respectively. Since the resolution along a laser ablation track is greater (500 data points) than in the perpendicular direction (up to 35 data points from the parallel tracks, see lowest profiles in B, C), we carried out two maps focusing on the enamel with horizontal and vertical track directions. In the modern sample (RG), the Sr concentrations throughout the tooth are relatively uniform with little contrast between enamel and dentine, the dentine-enamel junction (DEJ) is barely identifiable in the Sr maps. Towards the buccal enamel boundary (BEB) there is a moderate decrease in the Sr concentrations. The U and Th concentrations are all close to the detection limit of 0.1 ppb for our particular analytical setup. The Zn distribution shows a clear contrast between enamel and dentine, but also an outer rim in the enamel with high concentrations (D). Where the occlusal surface of the tooth is worn this is also evident by the absence of the Zn rim (vertical tracks 8 to 16, cycles 100 to 200). The Zn rim in the enamel can be geochemically used to identify erosion of the enamel surface, which would facilitate diagenetic alteration (Eggins et al., 2003).

The U and Th distributions in the Neanderthal tooth (Payre 1) have previously been mapped by Grün et al. (2008). Fig. 1 shows maps of Sr (Fig. 1B, C) and U concentrations (Fig. 1D, E). In contrast to the modern sample (Fig. 2), Sr concentrations in the Neanderthal tooth vary significantly between dentine and enamel. In dentine they are between 150 and 250 ppm, whereas in enamel, they are around 60–110 ppm. The Sr concentrations also show a clear separation at the DEJ. There is a gradient in Sr concentration from the dentine that is not covered with enamel towards the interior of the tooth (see arrow in Fig. 1C). The enamel has somewhat elevated Sr concentrations near the base (solid ellipse in Fig. 1C) and low concentrations near the outer surface (e.g. area of the dotted ellipse in Fig. 1C). The general concentration gradients of Sr and U are similar, and even smaller features of concentration changes are reproduced (compare circled sections in track 3, or details in track 6). Since virtually all measured U is the result of post depositional U-uptake, we interpret the co-varying distribution of Sr in dentine to reflect post depositional Sr uptake.

In contrast to dentine, there are both similarities as well as clear differences between the U and Sr distributions in the enamel. Both Sr and U are enriched at the base of the enamel (solid ellipses in Fig. 1C and E), and depleted close to the outer surface (dotted ellipses in Fig. 1C and E). However, U is enriched along lineaments, and in a central patch (see rectangle in Fig. 1D and track 13), while Sr does not show any apparent concentration changes in these areas (Fig. 1C and track 13). Furthermore, U concentrations drop by a factor of 25–100 at the DEJ while the Sr concentrations drop by a factor of 2–3. The Sr concentrations in the detrital material on the outside of the enamel are less than twice the Sr inside the enamel while the U contrast is in the range of 100. Fig. 3 shows the Zn and Th maps for the Neanderthal tooth. The Zn rim is completely intact for the tooth (Fig. 3A) showing that no abrasion or material removal through weathering has taken place. Th only occurs within a very small volume on the surface of the tooth and is an indicator of remaining sediment and other surface contaminations (Fig. 3B).

Fig. 4 details the relationship between Sr and U concentrations in the different enamel domains of the Neanderthal tooth (Payre 1). While the U concentrations vary over 5 orders of magnitude, Sr varies only by a factor of 2–4. The enamel was subdivided into four different domains. The outside domain is the volume of enamel immediately on the interior of the Th peaks to a depth of about 50 μm (see Fig. 3B, track 4 and track 12). The BEB domain corresponds to the volume with increased Zn concentrations (Fig. 3A, track 4 and track 12). The base

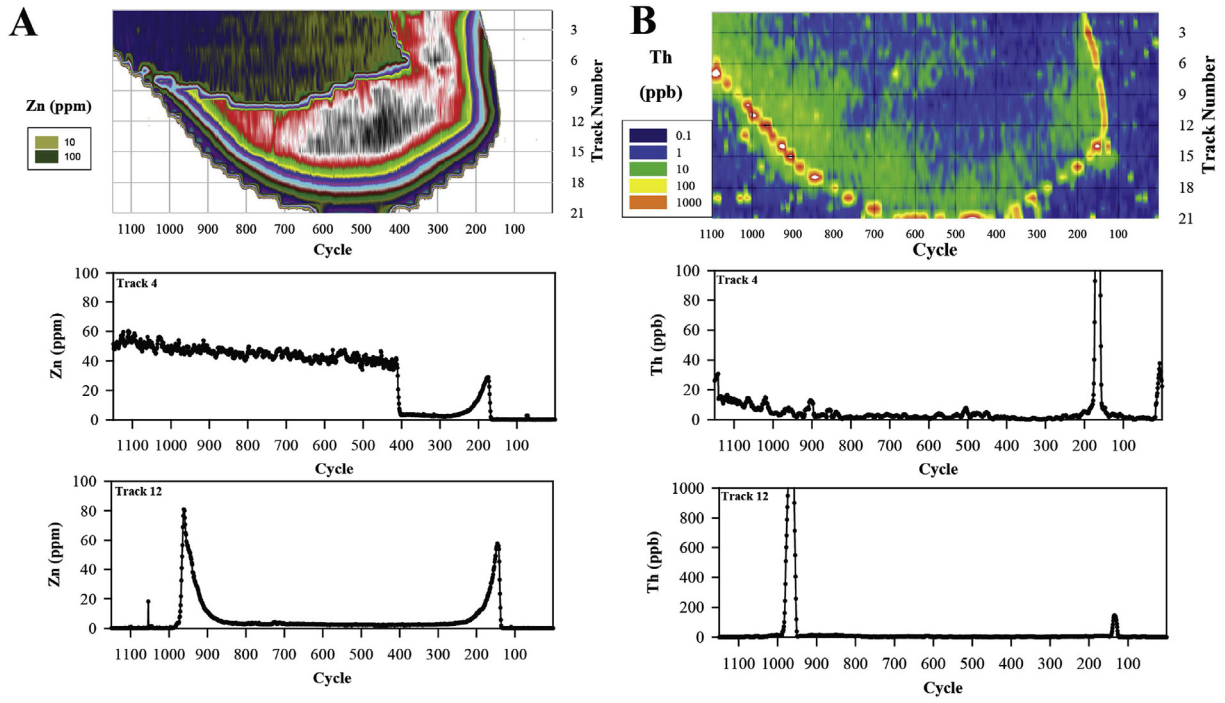

Fig. 3. A: Zn distribution map (planar view) and selected tracks, B: Th distribution map (planar view) and selected tracks, of the Neanderthal tooth (Payre 1).

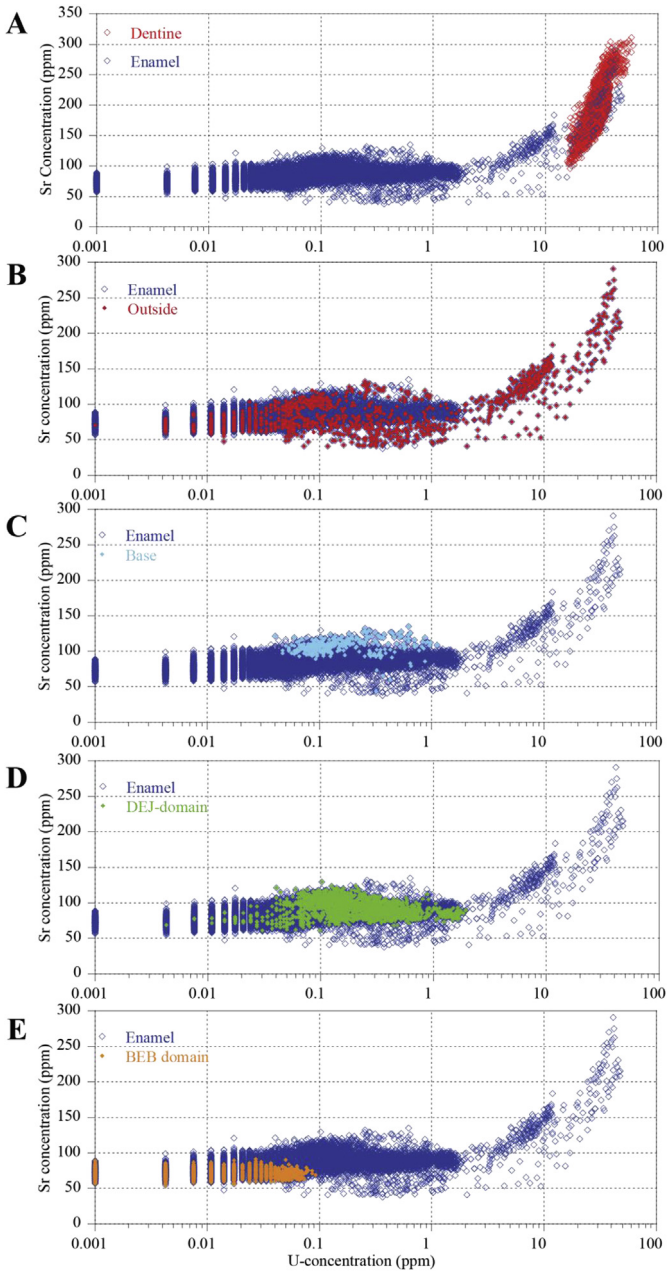

Fig. 4. Relationship of Sr and U concentrations in different domains of the Neanderthal tooth (Payre 1); Enamel, Dentine, Base, Dentine-enamel junction (DEJ), buccal enamel boundary (BEB).

domain relates to the area with increased Sr and U concentrations (solid circles in Fig. 1C and E), and the DEJ domain contains the remaining data points. It can be seen that all high U and Sr concentrations occur in the surface veneer (Fig. 4B) and are the result of diffusion from the outside. The base domain (Fig. 4C) has the highest Sr concentrations in the enamel, followed by the DEJ domain (Fig. 4D). The BEB domain has the lowest U and Sr concentrations and is thus least influenced by diagenesis (Fig. 4E). This means that on the one hand, U can be used to identify domains that contain original Sr isotope signatures, on the other hand, if no such low U domains can be identified, it will be impossible to ascertain whether any Sr analysis provided non-contaminated results. As soon as the outer surface of the enamel is weathered, U-migration proceeds from the outside (Eggins et al., 2003). Such teeth will be rendered unsuitable for Sr isotopic analysis.

The effect of diagenetic overprint is illustrated in Fig. 5. $^{87}Sr/^{86}Sr$ isotope ratio analysis using micro-drilling TIMS yielded a value of 0.7087 for the dentine. Three of the enamel $^{87}Sr/^{86}Sr$ ratios are closely similar, around 0.7108, while the forth is significantly lower at 0.7097. The latter was drilled from the domain with highly elevated U-concentrations (rectangle in Fig. 1E), and shows a diagenetic overprint from the dentine, lowering the $^{87}Sr/^{86}Sr$ ratio by around 0.0011.

3.2. *Investigating the accuracy of strontium isotope measurements by LA-MC-ICP-MS*

In 2007, we created a distribution map of $^{87}Sr/^{86}Sr$ ratios for the Neanderthal tooth (Payre 1) with the aim of resolving changes in diet and mobility from the diagenetic overprint. We found a large range of $^{87}Sr/^{86}Sr$ ratios of 0.707–0.710 for dentine and 0.712–0.718 for enamel (Fig. 6). Initially, this was interpreted as diagenetic overprint with the end members reflecting the $^{87}Sr/^{86}Sr$ composition of the Jurassic limestone, the bedrock where the tooth was found, and a $^{87}Sr/^{86}Sr$ ratio of around 0.718, thought to be the isotopic signature of the region of origin of this individual (Fig. 6D). However, further investigations showed that the $^{87}Sr/^{86}Sr$ isotope ratios obtained by LA-MC-ICP-MS, especially in the enamel, are much higher than the $^{87}Sr/^{86}Sr$ isotope ratios determined by micro-drilling TIMS. In conjunction with the observed correlation between increasing $^{87}Sr/^{86}Sr$ ratios and decreasing Sr concentrations (Fig. 6D) this points to a bias stemming from analytical interferences, most likely the previously identified polyatomic interference on mass 87 (Horstwood et al., 2008; Lewis et al., 2014; Simonetti et al., 2008). This example illustrates that monitoring and, if necessary correcting for this analytical bias, is critical for any interpretation of

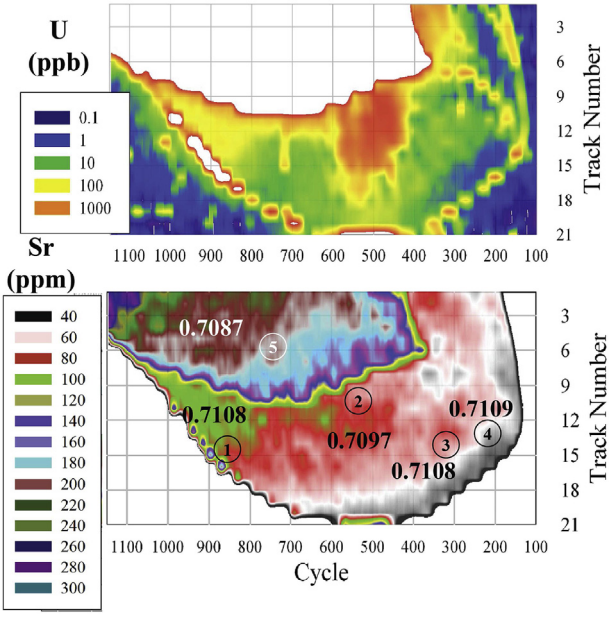

Fig. 5. U and Sr elemental concentration map and $^{87}Sr/^{86}Sr$ isotopic composition at 5 locations determined by TIMS analysis from the Neanderthal tooth Payre 1. There is a direct relationship between diagenetic overprint as indicated by elevated U concentrations at location 2 and a shift in $^{87}Sr/^{86}Sr$ isotope ratio.

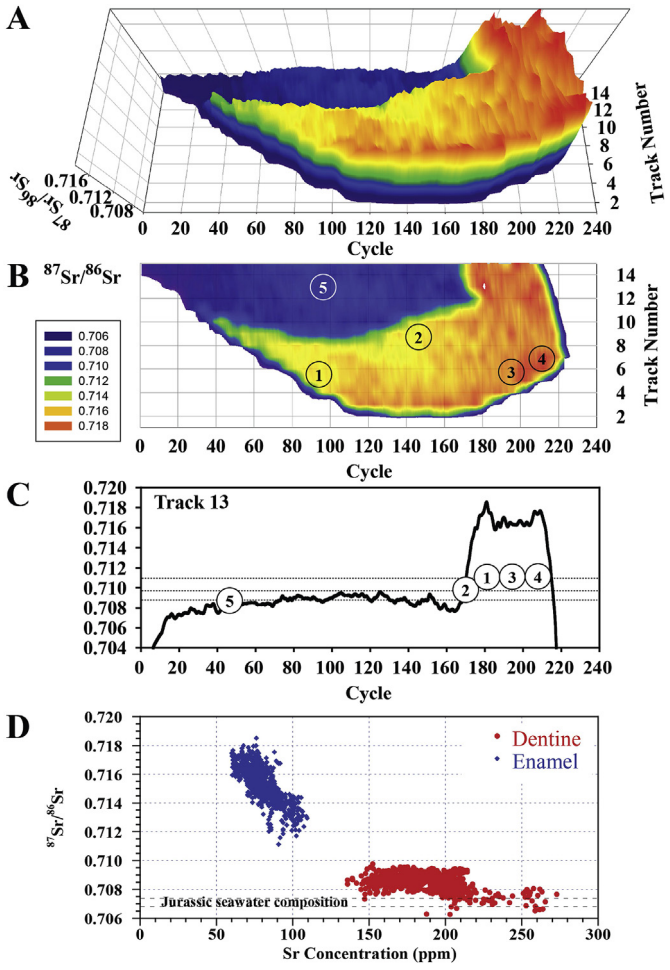

Fig. 6. A, B: Distribution map of the $^{87}Sr/^{86}Sr$ ratios of the Neanderthal tooth (Payre 1) in oblique and planar view, circles show the positions of the solution TIMS analyses. C: Track 13 with a projection of the TIMS analysis spots and their corresponding $^{87}Sr/^{86}Sr$ ratios. D: Differences between Sr concentrations and $^{87}Sr/^{86}Sr$ ratios in the enamel and dentine.

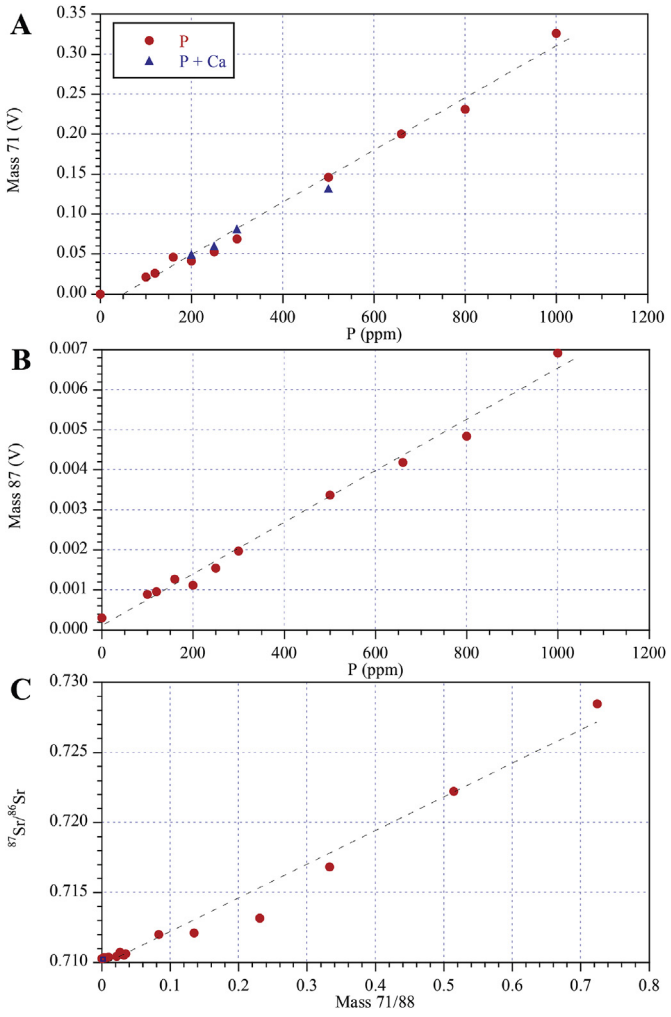

Fig. 7. A: Signal intensity of Mass 71 (V) plotted against P concentration, B: Signal intensity of Mass 87 (V) caused by the interference plotted against P concentration. P + Ca not shown because the Ca standard contains traces of Sr. C: SRM987 mixed with various P concentrations. Blue square indicates the value of SRM987 without any added P measured during this analytical session 0.71024 ± 2 (n = 8, 2σ). (For interpretation of the references to colour in this figure legend, the reader is referred to the web version of this article.)

strontium isotope ratios from teeth in terms of diagenetic overprint or mobility.

3.2.1. *The polyatomic interference on mass 87*

A polyatomic interference on mass 87 is suggested to be the main cause of observed offsets between solution and *in situ* analyses of $^{87}Sr/^{86}Sr$ isotope ratios in teeth, observed in many analytical facilities. This interference has been described in the literature as $^{40}Ca^{31}P^{16}O$ (Horstwood et al., 2008; Simonetti et al., 2008). However, a $^{40}Ar^{31}P^{16}O$ interference is also possible as Ar is always present in analysis on a MC-ICP-MS. In order to determine whether this interference originates from Ca or Ar we used solutions of ultra-clean nitric acid mixed with Ca and P in varying concentrations and monitored masses 71 (^{40}Ca or ^{40}Ar, ^{31}P) and 87 (^{40}Ca or ^{40}Ar, $^{31}P^{16}O$). Fig. 7A, B shows that there is a positive correlation between P concentration and the voltage produced on mass 71 and 87. No difference was observed, whether the solutions contained Ca or not (Fig. 7). This indicates that the polyatomic interference is related to Ar rather than Ca and provides direct evidence of the $^{40}Ar^{31}P^{16}O$ polyatomic compound. Fig. 7C shows the effect on the measured Sr isotope ratio of the standard solution SRM987, with increasing P concentrations. We observe increasing deviations from the accepted value of this standard, which in the absence of other interferences, are directly attributable to the $^{40}Ar^{31}P^{16}O$ polyatomic compound. Furthermore, in solution analysis, there is a direct relationship between increasing 71/88 ($^{40}Ar^{31}P$), as a measure of relative P to Sr concentration, and the deviation from the accepted $^{87}Sr/^{86}Sr$ isotope ratio of SRM987. This suggests that mass 71 could be used to monitor and correct the polyatomic interference on 87. At 71/88 ratios of >0.05, significant offsets are observed and as the 71/88 voltage increases, the observed offset increases reaching values of 0.03, dominating the $^{87}Sr/^{86}Sr$ ratio at high P concentrations (Fig. 7C). The effect of the interference on the $^{87}Sr/^{86}Sr$ ratio is hypothesised to be essentially controlled by the Sr concentration and oxide production rate, which in turn depends on the specific analytical facility used and the instrument conditions during analysis. Both Ca and P are stoichiometric components in bioapatite, and Ar is always present in the plasma, and thus can

be assumed to be constant.

3.2.2. Correcting for the polyatomic interference

To mitigate the bias arising from the polyatomic interference it is necessary to either reduce the oxide levels (Foster and Vance, 2006; Lewis et al., 2014), to apply a correction for the interference by using a suitable proxy, or a calibration with known sample materials (Horstwood et al., 2008).

The oxide production rate during laser ablation MC-ICP-MS analysis depends on the instrument tuning conditions, and the material and element being analysed (i.e. on the metal - oxide bond strength). Changes in oxide levels caused by the different tuning of the instrument can be monitored for example by measuring UO^+/U^+, in NIST 610 or in a U bearing solution. Horstwood et al. (2008) found an UO^+/U^+ production rate of 0.25%–1% using a U-solution and oxide production rates of 2.8% during laser ablation analysis. The oxide production rate is different for solution and laser ablation MC-ICP-MS analyses and is not directly transferable between different analytical setups. It varies greatly between different instruments and analytical facilities. Assuming that the blank corrected voltage on mass 87 in the ultra-clean nitric acid solution is solely caused by the oxide, it is possible to calculate an average oxide production rate from mass 71 ($^{40}Ar + {}^{31}P$) to mass 87 ($^{40}Ar + {}^{31}P + {}^{16}O$) of 2.2 ± 0.56% (n = 10, 2σ) for the solution analysis conducted at our facility. We find no positive linear correlation (r = −0.64) between the increase in P concentration and changes in oxide production rate in our solution analysis (Fig. 8).

LA-MC-ICP-MS analysis of NIST 610 and monitoring of UO^+/U^+ shows that the oxide production rate is highly dependent on the instrument conditions. Tuning for maximum signal intensity of ^{88}Sr showed UO^+/U^+ production rates of ~1%, but depending on the tuning, rates of up to 7.5% were possible. The oxide production depends on the residence time of the particles in the plasma and thus sample gas flow and position of the torch are hypothesised to be the most sensitive tuning parameter. A low sample gas flow allows the plasma to break down oxides more efficiently, but comes at the expense of decreased signal intensity. This can be countered by adding nitrogen to the plasma, which increases the energy distribution into the central channel, resulting in a higher signal intensity. Adding 8 cc/min nitrogen allows the reduction of the sample gas flow by ~50%, significantly increasing the residence time of the particulates in the plasma. This reduces oxide production rates by 2 orders of magnitude while decreasing the ^{88}Sr intensity by only a factor of 2–3. Possible nitrogen based interferences were checked by running mass scans across the full Sr isotope mass range and none were found.

However, while the tuning of the LA-MC-ICP-MS can be kept the same between a series of analyses, the conditions in the plasma may change due to different loading conditions when analysing different samples. This means that the residual oxide production rate cannot assumed to be constant and may change between samples and should ideally be monitored independently. Since it is not possible to monitor $^{40}Ar + {}^{31}P + {}^{16}O$ directly, a proxy for the oxide production rate needs to be used, potentially mass 89 ($^{40}Ar + {}^{31}P + {}^{18}O$), but this has also potential REE interference. In addition, the error magnification from the $^{18}O/^{16}O$ ratio would make this correction problematic. Mass 103.9 ($^{88}Sr^{16}O$) could be used to determine the residual oxide production during each analysis, but the production of this oxide is extremely low and very close to the background level of 4.6×10^{-5} V, at Sr concentrations of ~300 ppm. Since a constant oxide production rate cannot be assumed, and no adequate independent monitor was found, it was not possible to correct for the potential residual oxide production rate using our analytical setup.

3.2.3. Improvement in accuracy

Tuning the instrument for reduced oxide production resulted in an average $\Delta_{LA\text{-}TIMS}$ value of 38 ± 394 ppm (n = 21, 2σ) for the human and animal teeth (Fig. 9 and Table 6). This is a significant improvement over our previously obtained data, which had an average $\Delta_{LA\text{-}TIMS}$ value of ~3700 ppm. In absolute terms, we now achieve an average $\Delta_{LA\text{-}TIMS}$ value of 0.00003 ± 0.00028 (n = 21, 2σ). Without tuning for reduced oxide production, the strontium isotope ratios acquired by *in situ* LA-MC-ICP-MS in our laboratory were dominated by the interference of the polyatomic compound. The analyses of the shark and dugong teeth show only minor differences between the different tuning protocols. This is because shark and dugong teeth have much higher Sr concentrations (>1000 ppm) than the human and terrestrial animal teeth (~100 s of ppm) and were thus not significantly influenced by the polyatomic interference. Applying the improved analytical protocol to the Neanderthal tooth (Payre 1) resulted in $^{87}Sr/^{86}Sr$ ratios of 0.70885 ± 10 (±2se) and 0.71084 ± 9 (±2se) for the dentine and enamel (next to spot 3), respectively. These new values are in agreement with the solution TIMS analysis with $^{87}Sr/^{86}Sr$ ratios of 0.70871 ± 8 (±2se) for the dentine, and 0.71094 ± 11 (±2se), 0.71080 ± 5 (±2se), 0.71081 ± 6 (±2se) for the enamel. In terms of

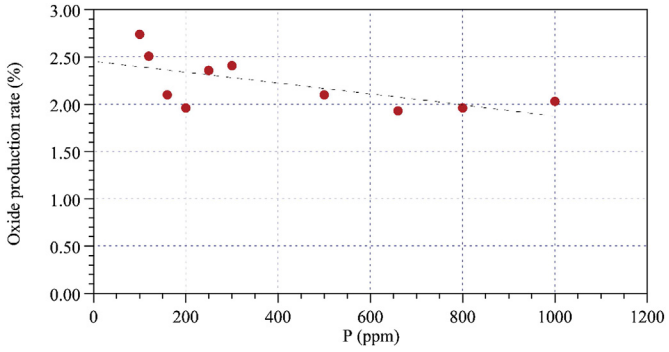

Fig. 8. Relationship between P concentration and oxide production rate during solution analysis using 2% nitric acid (r = −0.64).

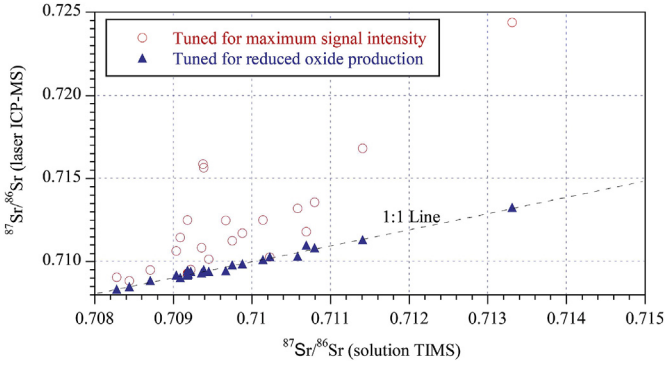

Fig. 9. Enamel and dentine samples analysed using LA-MC-ICP-MS with tuning for maximum signal intensity (circles) compared to tuning for reduced oxide production (diamonds). Spots for each analysis were directly bordering the TIMS drill spot of each samples used to determine the correct $^{87}Sr/^{86}Sr$ isotope ratio. Analytical errors are smaller than the size of the symbols.

Table 6
Summary of the TIMS and LA-MC-ICP-MS strontium isotope data for the human and animal tooth samples.

Sample details		TIMS		LA-MC-ICP-MS			LA-MC-ICP-MS 8 cc N					Absolute difference		Relative difference (ppm)	
Sample	Sample type	$^{87}Sr/^{86}Sr$	2se	Spot size (μm)	$^{87}Sr/^{86}Sr$	2se	88 (V)	71 (V)	104 (V)	$^{87}Sr/^{86}Sr$	2se	$\Delta_{LA\text{-}TIMS}$	$\Delta_{LA\text{-}TIMS}$ 8 cc N	$\Delta_{LA\text{-}TIMS}$	$\Delta_{LA\text{-}TIMS}$ 8 cc N
Tum SLMEM263	dentine	0.70967	0.00003	265	0.71248	0.00013	0.70	0.00440	0.00004	0.70945	0.00010	0.00281	−0.00022	3957	−313
Tum SLMEM466	dentine	0.71058	0.00004	265	0.71318	0.00020	0.45	0.00675	0.00005	0.71032	0.00021	0.00259	−0.00026	3650	−367
Tum SLMEM308	dentine	0.70918	0.00002	265	0.71249	0.00030	0.58	0.00534	0.00006	0.70947	0.00011	0.00332	0.00029	4676	407
Tum SLMEM308	enamel	0.70939	0.00001	265	0.71564	0.00029	0.72	0.00775	0.00003	0.70951	0.00010	0.00625	0.00012	8815	167
Tum SLMEM282	dentine	0.71014	0.00003	265	0.71249	0.00034	0.65	0.00799	0.00007	0.71012	0.00008	0.00236	−0.00002	3316	−23
Tum SLMEM282	enamel	0.71141	0.00001	265	0.71682	0.00059	0.44	0.00638	0.00007	0.71132	0.00017	0.00541	−0.00009	7609	−122
Tum SLMEM432	dentine	0.70936	0.00003	265	0.71083	0.00031	0.56	0.00464	0.00006	0.70932	0.00021	0.00147	−0.00004	2073	−58
Tum SLMEM432	enamel	0.70938	0.00008	265	0.71584	0.00054	0.42	0.00678	0.00003	0.70940	0.00009	0.00646	0.00002	9104	22
Tum SLMEM861	dentine	0.70988	0.00002	265	0.71170	0.00016	1.25	0.00791	0.00015	0.70986	0.00006	0.00182	−0.00002	2559	−31
Tum SLMEM1007	enamel	0.71331	0.00007	265	0.72437	0.00047	0.18	0.00524	0.00004	0.71326	0.00071	0.01106	−0.00005	15,505	−76
Tum SLMEM1251	dentine	0.70904	0.00016	265	0.71064	0.00031	0.90	0.00618	0.00005	0.70918	0.00008	0.00160	0.00013	2251	186
Bovid (1557)	enamel	0.70828	0.00002	265	0.70904	0.00015	2.15	0.00682	0.00016	0.70834	0.00005	0.00076	0.00006	1073	80
Bovid (1557)	dentine	0.70844	0.00002	265	0.70884	0.00008	5.21	0.00714	0.00016	0.70849	0.00002	0.00040	0.00005	566	68
Diprotodon (2104) molar	dentine	0.71023	0.00001	265	0.71026	0.00005	13.99	0.00572	0.00026	0.71029	0.00001	0.00003	0.00005	41	77
Neanderthal Payre 1	dentine	0.70871	0.00008	265	0.70948	0.00019	1.53	0.00959	0.00010	0.70885	0.00010	0.00077	0.00014	1083	204
Neanderthal Payre 1	enamel	0.71080	0.00005	265	0.71356	0.00020	1.05	0.00763	0.00010	0.71084	0.00009	0.00276	0.00004	3880	52
Neanderthal Payre 2	dentine	0.70945	0.00006	265	0.71015	0.00104	0.96	0.00818	0.00009	0.70939	0.00012	0.00070	−0.00006	988	−82
Neanderthal Payre 2	enamel	0.70909	0.00003	265	0.71144	0.00083	1.79	0.00764	0.00011	0.70902	0.00005	0.00235	−0.00007	3307	−101
Neanderthal Payre 3	dentine	0.70975	0.00002	265	0.71125	0.00033	1.86	0.00979	0.00012	0.70978	0.00006	0.00150	0.00003	2107	47
Neanderthal Payre 5	dentine	0.70922	0.00043	265	0.70951	0.00013	0.96	0.00818	0.00009	0.70939	0.00012	0.00029	0.00017	413	242
Neanderthal Payre 5	enamel	0.71069	0.00028	265	0.71179	0.00015	0.82	0.00772	0.00010	0.71099	0.00011	0.00110	0.00030	1543	425
Modern human (RG)	enamel			265	0.71280	0.00020	0.74	0.00826	0.00010	0.70987	0.00004				
Modern human (RG)	dentine			265	0.71091	0.00029	0.67	0.00760	0.00008	0.70995	0.00020				
											Mean	**0.00266**	**0.00003**	**3739**	**38**
Grey nurse shark		0.70918	0.00001	160	0.70927	0.00001	4.73	0.00258	0.00015	0.70918	0.00003	0.00009	0.00000	132	4
				160	0.70929	0.00002	4.78	0.00243	0.00014	0.70920	0.00004	0.00011	0.00002	158	32
				205	0.70926	0.00001	7.83	0.00485	0.00016	0.70922	0.00002	0.00008	0.00005	114	64
				205	0.70925	0.00001	10.85	0.00848	0.00031	0.70926	0.00001	0.00007	0.00008	105	108
Dugong		0.70918	0.00004	265	0.70923	0.00001	32.38	0.03099		0.70921	0.00001	0.00006	0.00003	78	49
				265	0.70922	0.00001	28.86	0.02882		0.70920	0.00001	0.00004	0.00002	57	30
				265	0.70923	0.00002	26.91	0.02951		0.70921	0.00001	0.00005	0.00003	76	47
Dugong		0.70919	0.00004	160	0.70927	0.00001	13.87	0.01665	0.00256	0.70925	0.00001	0.00008	0.00006	113	84
				160	0.70930	0.00002	12.14	0.01468	0.00211	0.70927	0.00002	0.00011	0.00008	157	112
											Mean	**0.00008**	**0.00004**	**110**	**59**

mobility, the original LA-MC-ICP-MS values of the enamel would have indicated a vastly different geologic substrate than those obtained by the new analytical protocol or with TIMS. With the new protocol our laser ablation data show both positive and negative offsets from the TIMS value. Fig. 10 shows increased $\Delta_{LA\text{-}TIMS}$ values at low 88 signal intensities, the result of less precise measurements at low signal intensities. There is a residual positive offset to higher $^{87}Sr/^{86}Sr$ ratios at high 88 signal intensities, indicating a residual production of the polyatomic interference of ~59 ppm, for samples > 1 V ^{88}Sr. The effect of the polyatomic compound does not correlate with the 71/88 ratio, which could have been a useful monitor as indicated by the solution analysis of SRM987 + P (comparison of Figs. 7C and 10). This is likely because P is a stoichiometric component of the bioapatite in teeth, and thus like Ca, and Ar from the gas, not limited during the analysis on a MC-ICP-MS. Since the isotopic composition in teeth may vary spatially, one expects to find both positive and negative $\Delta_{LA\text{-}TIMS}$ values because it was assumed that a single TIMS values was representative for that part of the tooth. This indicates that our improved analytical technique now allows the investigation of changes in $^{87}Sr/^{86}Sr$ ratios within a tooth. Finally, the $\Delta_{LA\text{-}TIMS}$ values now achieved in our lab (38 ± 394 ppm) are comparable to the results of Lewis et al. (2014), without the need of a customized plasma interface, though at a greater loss of signal intensity.

3.3. Analytical sampling strategies for fossil human teeth

The recent advancements of *in situ* laser ablation micro-analytical techniques made by a number of studies (Benson et al., 2013; Le Roux et al., 2014; Lewis et al., 2014) and in this research project significantly improve the application of this technique to fossil human teeth.

Scanning for diagenetic overprint can be rapidly applied to a large number of samples to identify teeth that have most likely preserved the original isotopic signatures. In an earlier paper we suggested to use laser ablation drilling for U-series micro-sampling (Benson et al., 2013). Fig. 11 shows how the laser can be used to probe the enamel BEB domain. The laser holes are 85 μm in diameter and cannot be seen with the naked eye (Fig. 11A). The uranium profiles can be used to identify the best locations for isotope analysis. From our study, we can develop the following sampling strategies for human teeth that keep any destruction to an absolute minimum. Firstly, the enamel is probed with an 85 μm laser spot for U, Th and Zn to estimate the depth of surface contamination (Th), to locate the BEB domain (Zn) and to evaluate diagenetic contamination (U). Once a suitable sample has been selected, different analytical methods can be applied to analyse its strontium isotopic composition.

In situ spot analysis for LA-MC-ICP-MS and micro-drilling for TIMS cause comparable damage (Fig. 11B), on the same scale as most surface impurities such as scratches, cracks and dirt. Micro-

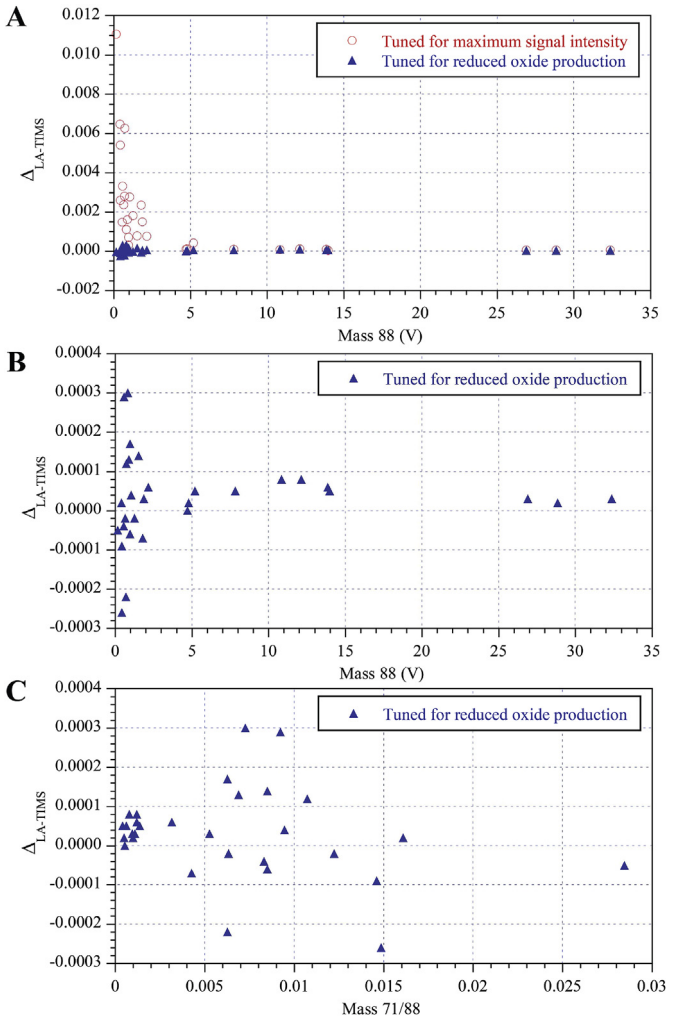

Fig. 10. A: $\Delta_{LA\text{-}TIMS}$ $^{87}Sr/^{86}Sr$ values for the complete dataset plotted against 88 (V), B: $\Delta_{LA\text{-}TIMS}$ values of the dataset tuned for reduced oxide production plotted against 88 (V), and C: plotted against 71/88.

drilling and TIMS analysis provides the most accurate results for the strontium isotope composition. However, for the study of intra-tooth isotopic variations, and a large number of samples, TIMS analysis can be prohibitively labour intensive and time consuming. In addition, TIMS analysis may average intra-tooth isotopic variation depending on the amount of material required and the size of the micro-drill. LA-MC-ICP-MS presents a valuable alternative because it allows for a high sample throughput, requires minimal sample preparation, and enables the investigation of intra-tooth isotopic variability at high spatial resolution. Intra-tooth isotopic variation can be investigated either along already broken surfaces, or possibly by sequential laser drilling similar to the U-series analysis (Benson et al., 2013).

The potential of the polyatomic interference on mass 87 during LA-MC-ICP-MS analysis varies between different analytical facilities. Changes in instrument conditions (laser cell design, gas sources, cones and torch design) can have a significant effect, and thus this interference should be monitored during each study. If present, tuning to minimise the oxide levels, is currently the most promising way for achieving accurate $^{87}Sr/^{86}Sr$ isotope ratio measurements from teeth using LA-MC-ICP-MS (this study, de Jong et al., 2007; Lewis et al., 2014). Monitoring and tuning to minimise $\Delta_{LA\text{-}TIMS}$ should be performed on a well characterised tooth standard with low Sr concentration (~100–300 ppm), in the same range as the unknown samples (e.g., Copeland et al., 2008, 2010; Le Roux et al., 2014).

Finally, the level of precision required to relate human samples to strontium isotope regions in the landscape will vary considerably between different geologic terrains. LA-MC-ICP-MS analysis with the accuracy range obtained here is sufficient for human mobility studies between most geologic terrains (e.g., Hodell et al., 2004; Evans et al., 2010; Frei and Frei, 2011; Bataille and Bowen, 2012; Willmes et al., 2014) and thus offers an alternative to solution analysis. This allows the application of this method to a large range of archaeological samples, which in turn will significantly improve our understanding of human and animal mobility and ranging patterns in the past.

4. Conclusions

The main conclusions from this project are:

(1) Using *in situ* LA-ICP-MS for U, Th, Sr and Zn concentrations in fossil teeth allows for rapid screening to identify zones of least diagenetic overprint. This method limits damage to the sample and ensures that only suitable samples are further processed for isotopic analysis.

(2) The polyatomic interference on mass 87 is the principal cause for the offset between solution and LA-MC-ICP-MS strontium isotope analysis observed in a significant number of analytical facilities. We found direct evidence that this interference originates from Ar, rather than Ca compounds. The effect of the interference on the $^{87}Sr/^{86}Sr$ isotope ratio is essential controlled by the Sr concentration and oxide production rate, because both Ca and P are stoichiometric

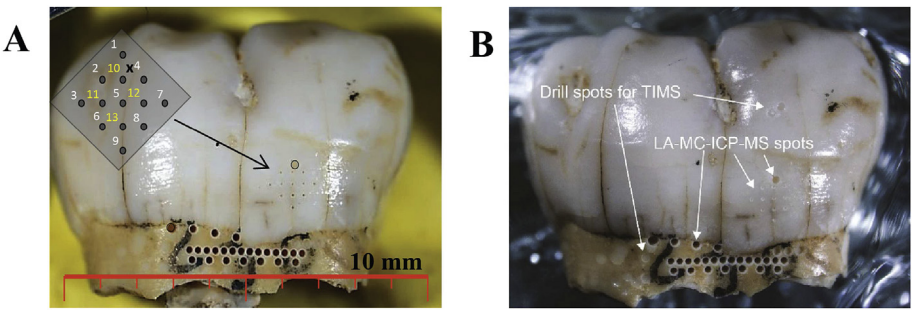

Fig. 11. Neanderthal tooth from Moula-Guercy (Benson et al., 2013) as an example of the overall damage caused to a tooth for isotopic analysis. A before and B after strontium isotope analysis by LA-MC-ICP-MS and drilling for solution TIMS. The row of holes in the dentine were used for U-series dating and are not related to the strontium isotope analysis.

components in bioapatite, and Ar is always present in the plasma.

(3) The oxide production rate in LA-MC-ICP-MS analysis varies between different analytical facilities, analytical conditions of the instrument, and the sample being analysed. No suitable proxy was found in this study to determine the oxide production rate during the analysis of a tooth independently, prohibiting online correction of potential oxide related interferences.

(4) Monitoring for this interference, and if present, tuning for reduced oxide levels is currently the most promising way to obtain accurate $^{87}Sr/^{86}Sr$ isotope ratio measurements from teeth using LA-MC-ICP-MS. We achieved $\Delta_{LA\text{-}TIMS}$ values of 38 ± 394 ppm (n = 21, 2σ). This analytical offset is small, particularly when considering the variability of $^{87}Sr/^{86}Sr$ isotope ratios in the environment.

(5) LA-MC-ICP-MS analysis of fossil human teeth can be used to investigate intra-tooth strontium isotopic variability and relate it to diagenetic alteration or changes in food source, thus providing a powerful technique to investigate diet and mobility patterns in archaeology.

Acknowledgements

The Grey Nurse Shark tooth was provided from the Australian Museum Sydney (Mark McGrouther) and the Dugong tooth from School of Archaeology and Anthropology, ANU (Colin Groves) This study was funded through ARC Discovery Grants DP0664144 (Grün et al.) *Microanalysis of human fossils: new insights into age, diet and migration* and DP110101415 (Grün et al.) *Understanding the migrations of prehistoric populations through direct dating and isotopic tracking of their mobility patterns*. We extend our thanks to Graham Mortimer, Ben Tranter, and the people of the Engineering workshop at RSES for their immense help with this project. Finally, we would like to thank two anonymous reviewers for their comments, which greatly improved this manuscript.

References

Ash, M.M., Nelson, S.J., 2003. Wheeler's Dental Anatomy, Physiology, and Occlusion, eighth ed. W.B. Saunders, Philadelphia.

Balasse, M., 2002. Reconstructing dietary and environmental history from enamel isotopic analysis: time resolution of intra-tooth sequential sampling. Int. J. Osteoarchaeol. 12, 155–165. http://dx.doi.org/10.1002/oa.601.

Balasse, M., Ambrose, S.H., Smith, A.B., Price, T.D., 2002. The seasonal mobility model for prehistoric herders in the south-western cape of South Africa assessed by isotopic analysis of sheep tooth enamel. J. Archaeol. Sci. 29, 917–932. http://dx.doi.org/10.1006/jasc.2001.0787.

Bataille, C.P., Bowen, G.J., 2012. Mapping 87Sr/86Sr variations in bedrock and water for large scale provenance studies. Chem. Geol. 304–305, 39–52. http://dx.doi.org/10.1016/j.chemgeo.2012.01.028.

Beard, B.L., Johnson, C.M., 2000. Strontium isotope composition of skeletal material can determine the birth place and geographic mobility of humans and animals. J. Forensic Sci. 45, 1049–1061.

Benson, A., Kinsley, L., Willmes, M., Defleur, A., Kokkonen, H., Mussi, M., Grün, R., 2013. Laser ablation depth profiling of U-series and Sr isotopes in human fossils. J. Archaeol. Sci. 40, 2991–3000. http://dx.doi.org/10.1016/j.jas.2013.02.028.

Bentley, R.A., 2006. Strontium isotopes from the earth to the archaeological skeleton: a review. J. Archaeol. Method Theory 13, 135–187. http://dx.doi.org/10.1007/s10816-006-9009-x.

Boel, C.A., 2011. Identifying Migration: Strontium Isotope Studies on an Early Bell Beaker Population from Le Tumulus des Sables, France. B.Sc. (Hons) Thesis. The Australian National University.

Britton, K., Grimes, V., Dau, J., Richards, M.P., 2009. Reconstructing faunal migrations using intra-tooth sampling and strontium and oxygen isotope analyses: a case study of modern caribou (Rangifer tarandus granti). J. Archaeol. Sci. 36, 1163–1172. http://dx.doi.org/10.1016/j.jas.2009.01.003.

Budd, P., Montgomery, J., Barreiro, B., Thomas, R.G., 2000. Differential diagenesis of strontium in archaeological human dental tissues. Appl. Geochem. 15, 687–694. http://dx.doi.org/10.1016/S0883-2927(99)00069-4.

Burton, J.H., Wright, L.E., 1995. Nonlinearity in the relationship between bone Sr/Ca and diet: paleodietary implications. Am. J. Phys. Anthropol. 96, 273–282. http://dx.doi.org/10.1002/ajpa.1330960305.

Capo, R.C., Stewart, B.W., Chadwick, O.A., 1998. Strontium isotopes as tracers of ecosystem processes: theory and methods. Geoderma 82, 197–225. http://dx.doi.org/10.1016/S0016-7061(97)00102-X.

Charlier, B.L.A., Ginibre, C., Morgan, D., Nowell, G.M., Pearson, D.G., Davidson, J.P., Ottley, C.J., 2006. Methods for the microsampling and high-precision analysis of strontium and rubidium isotopes at single crystal scale for petrological and geochronological applications. Chem. Geol. 232, 114–133. http://dx.doi.org/10.1016/j.chemgeo.2006.02.015.

Copeland, S.R., Sponheimer, M., de Ruiter, D.J., Lee-Thorp, J.A., Codron, D., le Roux, P.J., Grimes, V., Richards, M.P., 2011. Strontium isotope evidence for landscape use by early hominins – supplementary information. Nature 474, 76–78. http://dx.doi.org/10.1038/nature10149.

Copeland, S.R., Sponheimer, M., le Roux, P.J., Grimes, V., Lee-Thorp, J.A., de Ruiter, D.J., Richards, M.P., 2008. Strontium isotope ratios (87Sr/86Sr) of tooth enamel: a comparison of solution and laser ablation multicollector inductively coupled plasma mass spectrometry methods. Rapid Commun. Mass Spectrom. 22, 3187–3194. http://dx.doi.org/10.1002/rcm.3717.

Copeland, S.R., Sponheimer, M., Lee-Thorp, J.A., le Roux, P.J., de Ruiter, D.J., Richards, M.P., 2010. Strontium isotope ratios in fossil teeth from South Africa: assessing laser ablation MC-ICP-MS analysis and the extent of diagenesis. J. Archaeol. Sci. 37, 1437–1446. http://dx.doi.org/10.1016/j.jas.2010.01.003.

Courtaud, P., Chancerel, A., Cieselski, E., 2010. Le tumulus des Sables: Rapport de fouille programmée. Direction Régionale Commune de St-Laurent-Médoc. Les Affaires Culturelles d'Aquitaine Service Régional de l'Archéologie.

de Jong, H.N., Foster, G.L., Hawkesworth, C., Pike, A.W.G., 2007. LA-MC-ICPMS 87Sr/86Sr on tooth enamel—pitfalls and problems. Geochim. Cosmochim. Acta A 212.

Duval, M., Aubert, M., Hellstrom, J., Grün, R., 2011. High resolution LA-ICP-MS mapping of U and Th isotopes in an early Pleistocene equid tooth from Fuente Nueva-3 (Orce, Andalusia, Spain). Quat. Geochronol. 6, 458–467. http://dx.doi.org/10.1016/j.quageo.2011.04.002.

Eggins, S., Grün, R., Pike, A.W.G., Shelley, M., Taylor, L., 2003. 238U, 232Th profiling and U-series isotope analysis of fossil teeth by laser ablation-ICPMS. Quat. Sci. Rev. 22, 1373–1382. http://dx.doi.org/10.1016/S0277-3791(03)00064-7.

Eggins, S., Kinsley, L., Shelley, J.M.G., 1998. Deposition and element fractionation processes during atmospheric pressure laser sampling for analysis by ICP-MS. Appl. Surf. Sci. 127–129, 278–286. http://dx.doi.org/10.1016/S0169-4332(97)00643-0.

Elliott, J.C., 2002. Calcium phosphate biominerals. Rev. Min. Geochem. 48, 427–453. http://dx.doi.org/10.2138/rmg.2002.48.11.

Evans, J.A., Montgomery, J., Wildman, G., Boulton, N., 2010. Spatial variations in biosphere 87Sr/86Sr in Britain. J. Geol. Soc. Lond. 167, 1–4. http://dx.doi.org/10.1144/0016-76492009-090.

Fernandes, R., Hüls, M., Nadeau, M.-J., Grootes, P.M., Garbe-Schönberg, C.-D., Hollund, H.I., Lotnyk, A., Kienle, L., 2013. Assessing screening criteria for the radiocarbon dating of bone mineral. Nucl. Instrum. Methods Phys. Res. Sect. B Beam Interact. Mater. Atoms 294, 226–232. http://dx.doi.org/10.1016/j.nimb.2012.03.032.

Foster, G.L., Vance, D., 2006. In situ Nd isotopic analysis of geological materials by laser ablation MC-ICP-MS. J. Anal. At. Spectrom. 21, 288. http://dx.doi.org/10.1039/b513945g.

Frei, K.M., Frei, R., 2011. The geographic distribution of strontium isotopes in Danish surface waters – a base for provenance studies in archaeology, hydrology and agriculture. Appl. Geochem. 26, 326–340. http://dx.doi.org/10.1016/j.apgeochem.2010.12.006.

Grün, R., Aubert, M., Joannes-Boyau, R., Moncel, M.-H.H., 2008. High resolution analysis of uranium and thorium concentration as well as U-series isotope distributions in a Neanderthal tooth from Payre (Ardèche, France) using laser ablation ICP-MS. Geochim. Cosmochim. Acta 72, 5278–5290. http://dx.doi.org/10.1016/j.gca.2008.08.007.

Grün, R., Eggins, S., Kinsley, L., Moseley, H., Sambridge, M., 2014. Laser ablation U-series analysis of fossil bones and teeth. Palaeogeogr. Palaeoclimatol. Palaeoecol. 416, 150–167. http://dx.doi.org/10.1016/j.palaeo.2014.07.023.

Grün, R., Kinsley, L., Eggins, S., 2013. Maps of elemental distributions in modern and fossil human teeth. In: 7th Bone Diagenesis Meeting, pp. 22–25.

Hans, U., Kleine, T., Bourdon, B., 2013. Rb–Sr chronology of volatile depletion in differentiated protoplanets: BABI, ADOR and ALL revisited. Earth Planet. Sci. Lett. 374, 204–214. http://dx.doi.org/10.1016/j.epsl.2013.05.029.

Hinz, E.A., Kohn, M.J., 2010. The effect of tissue structure and soil chemistry on trace element uptake in fossils. Geochim. Cosmochim. Acta 74, 3213–3231. http://dx.doi.org/10.1016/j.gca.2010.03.011.

Hodell, D.A., Quinn, R.L., Brenner, M., Kamenov, G., 2004. Spatial variation of strontium isotopes (87Sr/86Sr) in the Maya region: a tool for tracking ancient human migration. J. Archaeol. Sci. 31, 585–601. http://dx.doi.org/10.1016/j.jas.2003.10.009.

Hoppe, K.A., Koch, P.L., Furutani, T.T., 2003. Assessing the preservation of biogenic strontium in fossil bones and tooth enamel. Int. J. Osteoarchaeol. 13, 20–28. http://dx.doi.org/10.1002/oa.663.

Horstwood, M.S.A., Evans, J.A., Montgomery, J., 2008. Determination of Sr isotopes in calcium phosphates using laser ablation inductively coupled plasma mass spectrometry and their application to archaeological tooth enamel. Geochim. Cosmochim. Acta 72, 5659–5674. http://dx.doi.org/10.1016/j.gca.2008.08.016.

Horwitz, E.P., Chiarizia, R., Dietz, M.L., 1992. A novel strontium-selective extraction chromatographic resin*. Solvent Extr. Ion. Exch. 10, 313–336. http://dx.doi.org/10.1080/07366299208918107.

Jackson, M., Hart, S.R., 2006. Strontium isotopes in melt inclusions from Samoan basalts: implications for heterogeneity in the Samoan plume. Earth Planet. Sci. Lett. 245, 260–277. http://dx.doi.org/10.1016/j.epsl.2006.02.040.

Jacques, L., Ogle, N., Moussa, I., Kalin, R., Vignaud, P., Brunet, M., Bocherens, H., 2008. Implications of diagenesis for the isotopic analysis of Upper Miocene large mammalian herbivore tooth enamel from Chad. Palaeogeogr. Palaeoclimatol. Palaeoecol. 266, 200–210. http://dx.doi.org/10.1016/j.palaeo.2008.03.040.

Jochum, K.P., Weis, U., Stoll, B., Kuzmin, D., Yang, Q., Raczek, I., Jacob, D.E., Stracke, A., Birbaum, K., Frick, D.A., Günther, D., Enzweiler, J., 2011. Determination of reference values for NIST SRM 610-617 glasses following ISO guidelines. Geostand. Geoanal. Res. 35, 397–429. http://dx.doi.org/10.1111/j.1751-908X.2011.00120.x.

Koenig, A.E., Rogers, R.R., Trueman, C.N., 2009. Visualizing fossilization using laser ablation-inductively coupled plasma-mass spectrometry maps of trace elements in Late Cretaceous bones. Geology 37, 511–514. http://dx.doi.org/10.1130/G25551A.1.

Kohn, M.J., Schoeninger, M.J., Barker, W.W., 1999. Altered states: effects of diagenesis on fossil tooth chemistry. Geochim. Cosmochim. Acta 63, 2737–2747. http://dx.doi.org/10.1016/S0016-7037(99)00208-2.

Konter, J.G., Storm, L.P., 2014. High precision 87Sr/86Sr measurements by MC-ICP-MS, simultaneously solving for Kr interferences and mass-based fractionation. Chem. Geol. 385, 26–34. http://dx.doi.org/10.1016/j.chemgeo.2014.07.009.

Le Roux, P.J., Lee-Thorp, J.A., Copeland, S.R., Sponheimer, M., de Ruiter, D.J., 2014. Strontium isotope analysis of curved tooth enamel surfaces by laser-ablation multi-collector ICP-MS. Palaeogeogr. Palaeoclimatol. Palaeoecol. http://dx.doi.org/10.1016/j.palaeo.2014.09.007.

Lewis, J., Coath, C.D., Pike, A.W.G., 2014. An improved protocol for 87Sr/86Sr by laser ablation multi-collector inductively coupled plasma mass spectrometry using oxide reduction and a customised plasma interface. Chem. Geol. 390, 173–181. http://dx.doi.org/10.1016/j.chemgeo.2014.10.021.

Longerich, H.P., Jackson, S.E., Günther, D., 1996. Laser ablation inductively coupled plasma mass spectrometric transient signal data acquisition and analyte concentration calculation. J. Anal. At. Spectrom. 11, 899–904. http://dx.doi.org/10.1039/Ja9961100899.

Martin, C., Bentaleb, I., Kaandorp, R., Iacumin, P., Chatri, K., 2008. Intra-tooth study of modern rhinoceros enamel δ18O: is the difference between phosphate and carbonate δ18O a sound diagenetic test? Palaeogeogr. Palaeoclimatol. Palaeoecol. 266, 183–189. http://dx.doi.org/10.1016/j.palaeo.2008.03.039.

Maurer, A.F., Galer, S.J.G., Knipper, C., Beierlein, L., Nunn, E.V., Peters, D., Tütken, T., Alt, K.W., Schöne, B.R., 2012. Bioavailable 87Sr/86Sr in different environmental samples – effects of anthropogenic contamination and implications for isoscapes in past migration studies. Sci. Total Environ. 433, 216–229. http://dx.doi.org/10.1016/j.scitotenv.2012.06.046.

McArthur, J.M., 1994. Recent trends in strontium isotope stratigraphy. Terra Nov. 6, 331–358. http://dx.doi.org/10.1111/j.1365-3121.1994.tb00507.x.

McArthur, J.M., Howarth, R.J., Bailey, T.R., 2001. Strontium isotope Stratigraphy: LOWESS version 3: best fit to the marine Sr-Isotope curve for 0–509 ma and accompanying look-up table for deriving numerical age. J. Geol. 109, 155–170. http://dx.doi.org/10.1086/319243.

McCormack, J.M., Bahr, A., Gerdes, A., Tütken, T., Prinz-Grimm, P., 2015. Preservation of successive diagenetic stages in Middle Triassic bonebeds: evidence from in situ trace element and strontium isotope analysis of vertebrate fossils. Chem. Geol. 410, 108–123. http://dx.doi.org/10.1016/j.chemgeo.2015.06.003.

Montgomery, J., Beaumont, J., Mackenzie, K., Gledhill, A., Shore, R., Brookes, S., Salmon, P., Lynnerup, N., 2012. Timelines in teeth: using micro-CT scans of partially mineralized human teeth to develop a new isotope sampling strategy. In: The 81st Annual Meeting of the American Association of Physical Anthropologists, Portland, Oregon, 216–216.

Montgomery, J., Evans, J.A., Cooper, R.E., 2007. Resolving archaeological populations with Sr-isotope mixing models. Appl. Geochem. 22, 1502–1514. http://dx.doi.org/10.1016/j.apgeochem.2007.02.009.

Moore, L.J., Murphy, T.J., Barnes, I.L., Paulsen, P.J., 1982. Absolute isotopic abundance ratios and atomic weight of a reference sample of strontium. J. Res. Natl. Inst. Stand. Technol. 87, 1–8. http://dx.doi.org/10.6028/jres.094.034.

Müller, W., Anczkiewicz, R., 2016. Accuracy of laser-ablation (LA)-MC-ICPMS Sr isotope analysis of (bio)apatite – a problem reassessed. J. Anal. At. Spectrom. 31, 259–269. http://dx.doi.org/10.1039/C5JA00311C.

Nanci, A., 2012. Ten Cate's Oral Histology: Development, Structure, and Function, eighth ed. Elsevier.

Nelson, B.K., Deniro, M.J., Schoeninger, M.J., De Paolo, D.J., Hare, P., 1986. Effects of diagenesis on strontium, carbon, nitrogen and oxygen concentration and isotopic composition of bone. Geochim. Cosmochim. Acta 50, 1941–1949. http://dx.doi.org/10.1016/0016-7037(86)90250-4.

Nowell, G.M., Horstwood, M.S.A., 2009. Comments on Richards et al., Journal of Archaeological Science 35, 2008 "Strontium isotope evidence of Neanderthal mobility at the site of Lakonis, Greece using laser-ablation PIMMS". J. Archaeol. Sci. 36, 1334–1341. http://dx.doi.org/10.1016/j.jas.2009.01.019.

Paton, C., Woodhead, J.D., Hergt, J.M., Phillips, D., Shee, S., 2007. Strontium isotope analysis of kimberlitic groundmass perovskite via LA-MC-ICP-MS. Geostand. Geoanal. Res. 321–330. http://dx.doi.org/10.1111/j.1751-908X.2007.00131.x.

Porat, N., Zhou, L.P., Chazan, M., Noy, T., Horwitz, L.K., 1999. Dating the lower paleolithic open-air site of Holon, Israel by luminescence and ESR techniques. Quat. Res. 51, 328–341. http://dx.doi.org/10.1006/qres.1999.2036.

Price, T.D., Blitz, J., Burton, J., Ezzo, J.A., 1992. Diagenesis in prehistoric bone: problems and solutions. J. Archaeol. Sci. 19, 513–529. http://dx.doi.org/10.1016/0305-4403(92)90026-Y.

Price, T.D., Burton, J.H.H., Bentley, R.A., 2002. The characterization of biologically available strontium isotope ratios for the study of prehistoric migration. Archaeometry 44, 117–135. http://dx.doi.org/10.1111/1475-4754.00047.

Richards, M., Grimes, V., Smith, C., Smith, T., Harvati, K., Hublin, J.J., Karkanas, P., Panagopoulou, E., 2009. Response to Nowell and Horstwood (2009). J. Archaeol. Sci. 36, 1657–1658. http://dx.doi.org/10.1016/j.jas.2009.03.009.

Rosman, K.J.R., Taylor, P.D.P., 1998. Isotopic compositions of the elements 1997 (technical report). Pure Appl. Chem. 70, 217–235. http://dx.doi.org/10.1351/pac199870010217.

Schoeninger, M.J., Hallin, K., Reeser, H., Valley, J.W., Fournelle, J., 2003. Isotopic alteration of mammalian tooth enamel. Int. J. Osteoarchaeol. 13, 11–19. http://dx.doi.org/10.1002/oa.653.

Sillen, A., Hall, G., Richardson, S., Armstrong, R., 1998. 87Sr/86Sr ratios in modern and fossil food-webs of the Sterkfontein Valley: implications for early hominid habitat preference. Geochim. Cosmochim. Acta 62, 2463–2473. http://dx.doi.org/10.1016/S0016-7037(98)00182-3.

Simonetti, A., Buzon, M.R., Creaser, R.A., 2008. In-situ elemental and Sr isotope investigation of human tooth enamel by Laser Ablation-(MC)-ICP-MS: successes and pitfalls. Archaeometry 50, 371–385. http://dx.doi.org/10.1111/j.1475-4754.2007.00351.x.

Slovak, N.M., Paytan, A., 2012. Handbook of environmental isotope geochemistry. Springer, Berlin, Heidelberg. http://dx.doi.org/10.1007/978-3-642-10637-8.

Sponheimer, M., Lee-Thorp, J.A., 1999. Alteration of enamel carbonate environments during fossilization. J. Archaeol. Sci. 26, 143–150. http://dx.doi.org/10.1006/jasc.1998.0293.

Suga, S., 1989. Enamel hypomineralization viewed from the pattern of progressive mineralization of human and monkey developing enamel. Adv. Dent. Res. 3, 188–198. http://dx.doi.org/10.1177/08959374890030021901.

Thirlwall, M.F., 1991. Long-term reproducibility of multicollector Sr and Nd isotope ratio analysis. Chem. Geol. Isot. Geosci. Sect. 94, 85–104. http://dx.doi.org/10.1016/0168-9622(91)90002-E.

Trickett, M.A., Budd, P., Montgomery, J., Evans, J., 2003. An assessment of solubility profiling as a decontamination procedure for the 87Sr/86Sr analysis of archaeological human skeletal tissue. Appl. Geochem. 18, 653–658. http://dx.doi.org/10.1016/S0883-2927(02)00181-6.

Trueman, C.N., Kocsis, L., Palmer, M.R., Dewdney, C., 2011. Fractionation of rare earth elements within bone mineral: a natural cation exchange system. Palaeogeogr. Palaeoclimatol. Palaeoecol. 310, 124–132. http://dx.doi.org/10.1016/j.palaeo.2011.01.002.

Trueman, C.N., Palmer, M.R., Field, J., Privat, K., Ludgate, N., Chavagnac, V., Eberth, D.A., Cifelli, R., Rogers, R.R., 2008. Comparing rates of recrystallisation and the potential for preservation of biomolecules from the distribution of trace elements in fossil bones. Comptes Rendus Palevol 7, 145–158. http://dx.doi.org/10.1016/j.crpv.2008.02.006.

Trueman, C.N., Tuross, N., 2002. Trace elements in recent and fossil bone apatite. Rev. Min. Geochem. 48, 489–521. http://dx.doi.org/10.2138/rmg.2002.48.13.

Vroon, P.Z., van der Wagt, B., Koornneef, J.M., Davies, G.R., 2008. Problems in obtaining precise and accurate Sr isotope analysis from geological materials using laser ablation MC-ICPMS. Anal. Bioanal. Chem. 390, 465–476. http://dx.doi.org/10.1007/s00216-007-1742-9.

Willmes, M., McMorrow, L., Kinsley, L., Armstrong, R., Aubert, M., Eggins, S., Falguères, C., Maureille, B., Moffat, I., Grün, R., 2014. The IRHUM (Isotopic Reconstruction of Human Migration) database – bioavailable strontium isotope ratios for geochemical fingerprinting in France. Earth Syst. Sci. Data 6, 117–122. http://dx.doi.org/10.5194/essd-6-117-2014.

Woodhead, J., Swearer, S., Hergt, J., Maas, R., 2005. In situ Sr-isotope analysis of carbonates by LA-MC-ICP-MS: interference corrections, high spatial resolution and an example from otolith studies. J. Anal. At. Spectrom. 20, 22. http://dx.doi.org/10.1039/b412730g.